December 2019

An Implementation of Fully Convolutional Network for Surface Mesh Segmentation

Taiyu Zhang
University of Wisconsin-Milwaukee

AN IMPLEMENTATION OF FULLY CONVOLUTIONAL NETWORK FOR SURFACE MESH SEGMENTATION

by

Taiyu Zhang

A Thesis Submitted in

Partial Fulfillment of the

Requirements for the Degree of

Master of Science

in Computer Science

at

The University of Wisconsin Milwaukee

December 2019

ABSTRACT

AN IMPLEMENTATION OF FULLY CONVOLUTIONAL NETWORK FOR SURFACE MESH SEGMENTATION

by

Taiyu Zhang

The University of Wisconsin Milwaukee, 2019
Under the Supervision of Professor Zeyun Yu

This thesis presents an implementation of a 3-Dimensional triangular surface mesh segmentation architecture named Shape Fully Convolutional Network, which is proposed by Pengyu Wang and Yuan Gan in 2018. They designed a deep neural network that has a similar architecture as the Fully Convolutional Network, which provides a good segmentation result for 2D images, on 3D triangular surface meshes. In their implementation, 3D surface meshes are represented as graph structures to feed the network. There are three main barriers when applying the Fully Convolutional Network to graph-based data structures.

- First, the pooling operation is much harder to apply to general graphs.
- Second, the convolution order on a graph structure is unstable.
- Third, the raw data of surface meshes cannot be directly applied to the network.

To solve these problems, first, all the nodes inside the graph are re-ordered into a 1-dimensional list based on a multi-level graph coarsening algorithm, which allows the pooling operation to be applied as easily as a 1D pooling. Second, a self-defined generating layer is added before each convolution layer in the network to generate the neighbors of each node on the graph, and at the same time, sort all neighbors based on the L2 similarity to keep the convolution operation in a stable manner. Finally, three translation and rotation free low-level geometric features are pre-processed and used as input to train the network. This Shape Fully Convolution Network can effectively learn and predict triangular face-wise labels. In the end, to achieve a better result, the final labeling is optimized by the multi-label graph cut algorithm, which gives punishment to the predicted result based on the smoothness of the surface. The experiments show that the model can effectively learn and predict triangle-wise labels on surface meshes and yields good segmentation results.

TABLE OF CONTENTS

LIST OF FIGURES

LIST OF TABLES

1. Introduction

The concept of segmentation is aiming to divide an object into some meaningful parts so that the internal structure of the object can be revealed. For segmentation on 2D images, labels are assigned to each pixel so the entire image can be divided into several significant components. The same idea is extended to 3D surface meshes. The segmentation on 3D surface meshes is to assign labels to each triangular face and, therefore, achieve the goal of segmentation. These labelings are very helpful in exploring the inherent characteristic of the shape. As some examples, the segmentation result can be applied to various fields of computer graphics, such as shape editing [1], shape deformation [2], and shape modeling [3]. These make the shape segmentation a research hotspot, but yet tricky in the fields of digital geometric model processing, and instance modeling persist.

Nowadays, the data-driven method, such as deep learning [4], becomes more and more popular in many areas. In the image processing area, convolutional neural networks have shown excellent performance in various image processing problems, such as image classification [5, 6, 7] which aims to predict an image as a whole into some specific classes; and semantic segmentation [8, 9, 10], which aims to predict pixel-wise classes. With the emerging encouraging study results, many researchers have devoted their efforts to various deformation studies on Convolutional Neural Networks. One of which is the Fully Convolutional Network [11]. This network can achieve end-to-end, pixel-to-pixel predictions on semantic image segmentation, with no requirements over the size of input images. Therefore, it has become one of the most popular methods for image segmentation. A couple of variations are build based on the Fully Convolutional Network architecture such as the DeConvNet [12], and U-Net [13]

Although the Fully Convolutional Network [11] can generate good results in 2D image segmentation, it can not be directly applied to 3D surface meshes. This mainly because of three reasons:

- First, unlike the 2D images where the data are stored as a 2D static array, which has a very standard data structure and regular neighborhood relationships. The surface meshes are stored by recording the coordinates for all vertices and the vertex indices for each triangular face. This particular data structure makes the regular pooling and convolution operation hard to apply.
- Second, in 2D images, each pixel has a well-organized neighborhood structure that has a fixed geometric order, where surface meshes do not have similar fixed neighborhood relationships. This un-structured neighborhood ordering may cause the convolution operation to become unstable.
- Third, the RGB data are globally well defined in a 2D image. In other words, a specific color is mapped to the same RGB values across any images. Therefore, it is safe to directly use the RGB value of an image as input data and let the network to figure out the high-level features. On the other hand, the coordinates of vertices or the surface normal of triangular faces are defined locally for each surface mesh, where the translation, such as zoom in and zoom out, and the rotation operation will change the coordinates and face normal for a surface mesh. This makes it unsafe to feed the network directly using the raw data of surface meshes.

A novel Shape Fully Convolutional Network [14] is designed based on the Fully Convolutional Network [11] to solve these problems. The Fully Convolutional Network has two main stages: a down-sampling path and an up-sampling path. The down-sampling path has a similar convolution and pooling architecture compare to the Deep Convolution Neural Network. Inspired by the Graph Convolutional Neural Network [15, 16, 17] where the convolution and pooling operation can be directly applied to an arbitrary graph. The same idea is extended to the Shape Fully Convolutional Network. Based on the design: First, three low-level geometric features are pre-processed and assigned to each triangular face in the surface mesh. Second, the 3D surface mesh is converted to a graph structure with each triangular face as a node and the neighborhood relationship between two faces as an edge. Third, before feeding the network, the graph is re-ordered into a 1D list based on the multi-level graph coarsening algorithm. Finally, a self-defined generating layer is added in the network before each convolution layer to generate the neighbors for convolution operation.

For the up-sampling path, the transpose-convolution operation proposed by the Fully Convolutional Network [11] is re-used. This operation provides a learnable way to optimize the up-sampling strategy. Moreover, the skip architecture from the Fully Convolutional Network is implemented, which passes the features from the down-sampling path to the up-sampling path at each level.

In the end, the prediction from the model is optimized base on a multi-label graph coarsening algorithm, which punishes the predicted labeling with the smoothness of the surface mesh. Figure 1 shows the pipeline of the model:

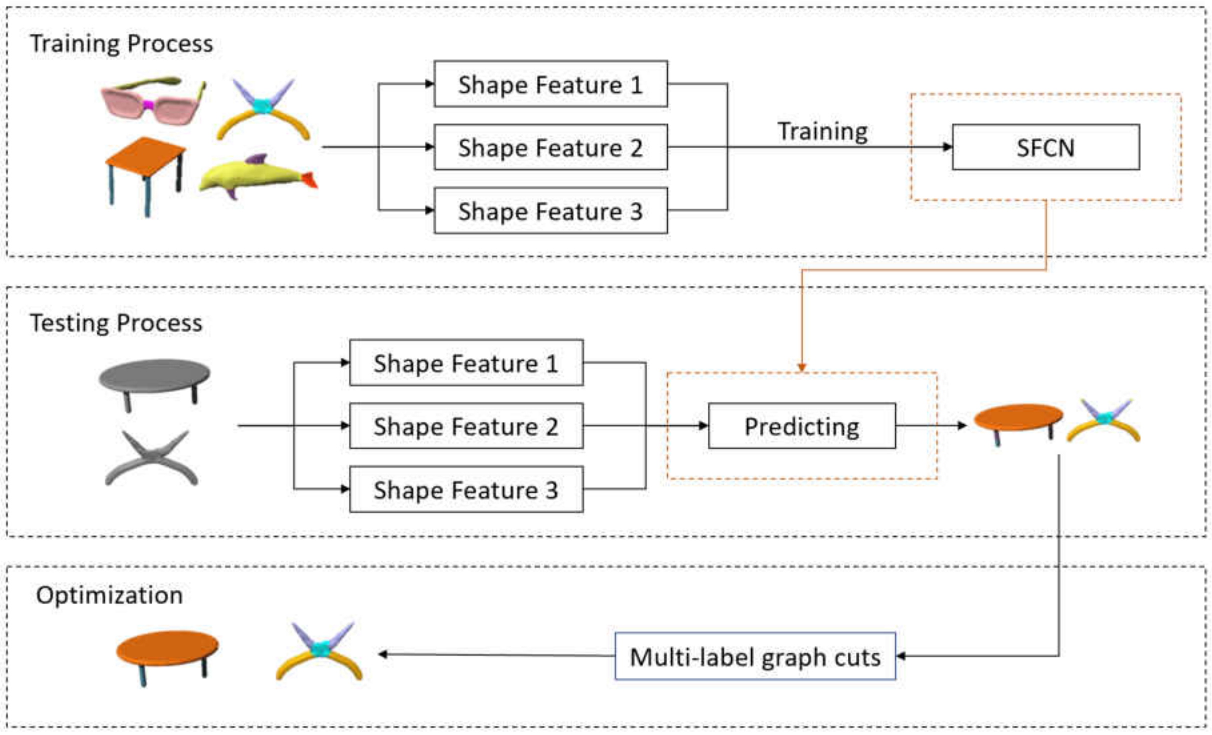

Figure 1 The pipeline of the Shape Fully Convolutional Network model [14]

This Shape Fully Convolution Network is able to train a triangles-to-triangles model for surface mesh segmentation, without any requirements on the triangle numbers of the input shape, and achieve good segmentation results.

2. Related Work

2.1. Fully Convolutional Network

The Fully Convolutional Network [11] proposed in 2015 is pioneering research that can effectively solve the problem of semantic image segmentation by pixel-level classification. It uses a down-sampling path that has a similar architecture as the Deep Convolution Neural Network, which is able to extract high-level features from the low-level RGB data. Then an up-sampling path based on the transpose convolution operating is attached to expand the coarsened features to the original image shape to achieve the pixel-wise prediction. A skip architecture that concatenates the coarsened high-level features in the up-sampling path with the finer low-level features from the down-sampling path is applied to the network to get a better result. Later, a great deal of research has emerged based on the Fully Convolutional Network algorithms and achieved good results in various fields such as edge detection [18], depth regression [19], optical flow [20], simplifying sketches [21], and etc.. However, the existing research on Fully Convolutional Network is mainly restricted to image processing, largely because image has a standard data structure, easy for convolution, pooling, and up-sampling operations.

2.2. Graphs Convolutional Neural Network

Standard Convolutional Neural Networks cannot work directly on data which have graph structures. However, there are some previous researches [16, 17, 22, 23] that discussed how to apply Convolutional Neural Networks on graph structures. Some of them [17, 22] use a spectral method by computing bases of the graph Laplacian matrix and perform the convolution in the spectral domain. Where one of the others [16] uses a PATCHY-SAN architecture, which maps from a graph representation onto a vector space representation by extracting locally connected regions from graphs based on a multi-level graph coarsening algorithm.

2.3. Deep Learning on 3D Shapes

The recent researches introduce various methods of deep convolutional architectures for 3D shapes. By using volumetric representation, which is proposed in the 3D ShapeNet [24] and the volumetric Convolution Neural Network [25], standard 2D convolution and pooling operation, or even augmentation methods can be easily extended to 3D data. However, data sparsity and the computation cost problem of 3D convolution has not yet been solved. The Projective Convolution Network [26] proposed a multi-view image-based Fully Convolutional Network and a surface-based Conditional Random Fields to do the 3D mesh labeling. Where the RGB data associated with the depth information of each pixel are used as input, however, it may need a lot of time to compute the surface-pixel reference, and more viewpoints to maximally cover the shape surface. Some other methods, such as the Synchronized Spectral Convolutional Neural Network [27] and the Point-net [28] proposed different deep architectures that can be trained directly on point clouds to achieve points segmentation and other 3D points analysis. However, the point cloud structure sampled from the original object surface may lack the intrinsic structure compare to surface mesh. For a better understanding of the intrinsic structures, many types of research directly adapt neural networks to surface meshes. The Geodesic Convolution Neural Network [29] used convolution filters in local geodesic polar coordinates. The Anisotropic Convolutional Neural Network [30] used anisotropic heat kernels as filters. The Mixture Model Convolutional Neural Network [31] considered a more generalized Convolutional Neural Network architecture by using the mixture model.

3. Shape Fully Convolutional Network

In 2018, Pengyu Wang and Yuan Gan proposed a 3-dimensional shape segmentation technique named Shape Fully Convolutional Network [14]. In this architecture, 3D triangular meshes are represented as graph structures with triangular faces as nodes and the neighborhood relationships as edges. Then the graph convolution and pooling operations proposed in the Graph Convolutional Neural Network [17] are applied to the graph, which is similar to convolutional and pooling operations used on 2D images. The graph is pre-ordered based on the multi-level coarsening algorithm [17], which allows the pooling operation much more comfortable to apply. Then a bridging function named generating operation [14] is designed that will generate proper neighborhood structures for each face to fit the convolution kernel. After the down-sampling path, the extracted features are then up-sampled using de-convolution operation and skip architecture proposed by the Fully Convolutional Network [11] that combines the feature from the same stage in the down-sampling path with the output of the de-convolution operation before passing to next stage. Finally, the prediction is optimized based on the multi-level graph cut algorithm [32].

3.1. Pooling Operation

Apply general convolution and pooling operation to graphs is not straightforward, because the general convolution and pooling are designed only for grid structures such as images. The major obstacles of applying them are to figure out the pooling order and convolution order. The pooling operation requires meaningful neighborhoods on graphs, where similar nodes are clustered together. However, finding out multiple levels of clustering is equivalent to finding out the multi-scale clustering of the graph, which is known as NP-hard [33]. Therefore, apply an approximation algorithm is much more practical.

3.1.1. Multi-level Graph Coarsening

To accurately approximate the multi-scale clustering, the coarsening phase proposed by the Graclus multilevel clustering algorithm [34] is applied, which has shown to be extremely efficient at clustering a large variety of graphs. Assume an input graph $G_0(V_0, E_0)$ with a set of vertices V_0 and a set of edges E_0 where each edge between two vertices represents their similarity. The goal for this coarsening phase is to transform the graph G_0 into a series of smaller and smaller graph $G_1, G_2, \cdots, G_m$ such that $|V_0| > |V_1| > \cdots > |V_m|$. The overview of multi-level coarsening is shown in figure 2.

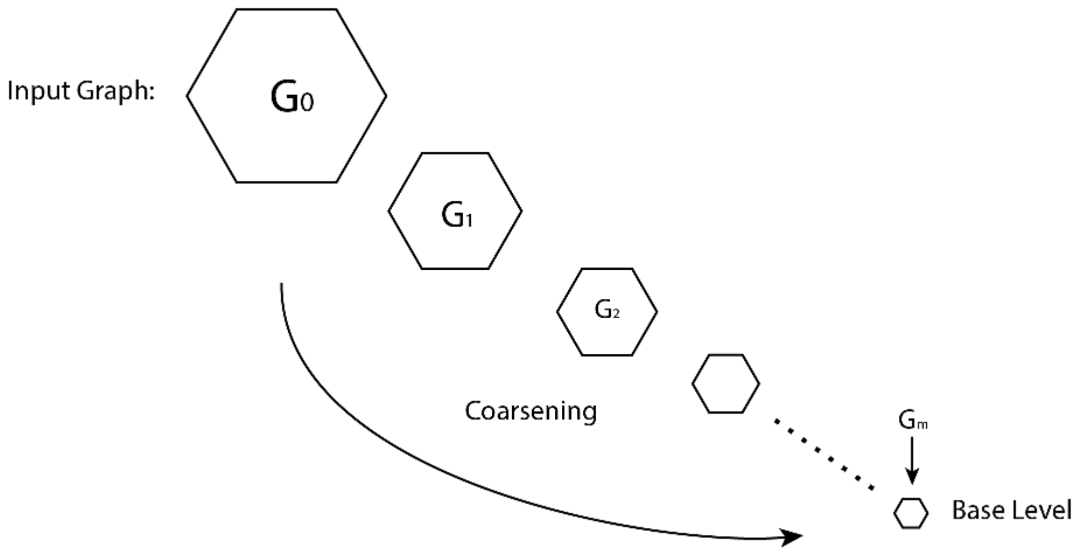

Figure 2 Overview of the Multilevel Coarsening [17]

For each level i, the algorithm is as follows: Start with all vertices un-marked. Visit each un-marked vertex $u \in V_i$ in random order, search for another unmarked vertex $v \in neighbor(u)$ such that u and v corresponds to the highest normalized weight

$$w(u,v) = \frac{e(u,v)}{d(u)} + \frac{e(u,v)}{d(v)}$$

among all neighbors. Then merge u and v, and set them as marked. If all neighbors of u have been marked, only mark u and do not merge it. In the equation, $e(u,v)$ corresponds to the edge weight between u and v. The higher the weight of the edge, the more likely the corresponding vertices would be clustered tighter. This edge weight should be normalized by $d(u)$, and $d(v)$, which are the degrees of vertex u and v. The degree of vertex u is defined as the summation of edge weights between u and all its neighbors

$$d(u) = \sum_{v \in neighbor(u)} e(u,v)$$

If $d(u)$ is low, it means that vertex u is unique in its neighborhood. It tends to not cluster with any neighbor. On the other hand, if $d(u)$ is high, it means that vertex u is similar to its neighborhood, and it can be clustered with more of its neighbors. By normalizing the edge weight by the degrees of the corresponding vertices, the coarsening algorithm can be applied to more general graphs.

3.1.2. Fast pooling based on coarsening

After coarsening, the vertices of the graph and its coarsened versions are not arranged in a way that pooling operation can be easily applied. However, it is possible to arrange the vertices such that a graph pooling operation can be as efficient as the 1D pooling. The output of the coarsening algorithm should be a binary tree with each parent corresponds to the merged nodes from its children. Each node would have either two children if it was matched at the finer level, or one, if it was not. Figure 3 shows an example of coarsening process and output. Suppose we carry out two layers of clustering. The original graph has 8 nodes. Then during the first clustering, node 4 and node 7 are leftover as singleton nodes. Therefore, node 2 and node 4 in layer 2 have only one child. During the second clustering, node 1 and node 2 are clustered together, and node 3 and node 4 are clustered together. Node 0 is leftover as a singleton, and therefore, node 0 in the base layer only has one child.

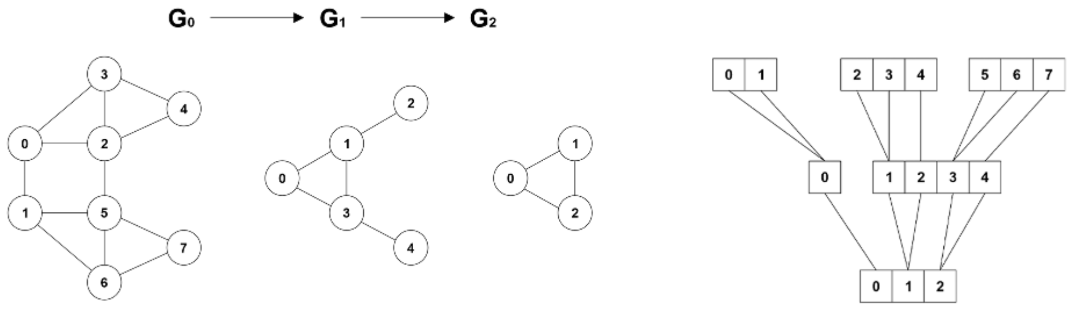

Figure 3 Example of coarsening output [17]

To get the proper pooling order, we need to re-arrange the tree structure returned from the coarsening phase into a balanced binary tree. From the base level to input level (coarsest level to finest level), fake nodes (disconnected nodes) are added to pair with the singletons so that each node should have two children:

1) regular nodes either have two regular nodes as children,
2) or one singleton and a fake node as children.
3) Fake nodes always have two fake nodes as children.

Suppose we carry out two layers of pooling with each pooling of size 2. Then two coarsening operations are needed. Based on figure 3, we then need to add fake nodes to make sure the output is a balanced binary tree. Figure 4 shows the pooling process and output.

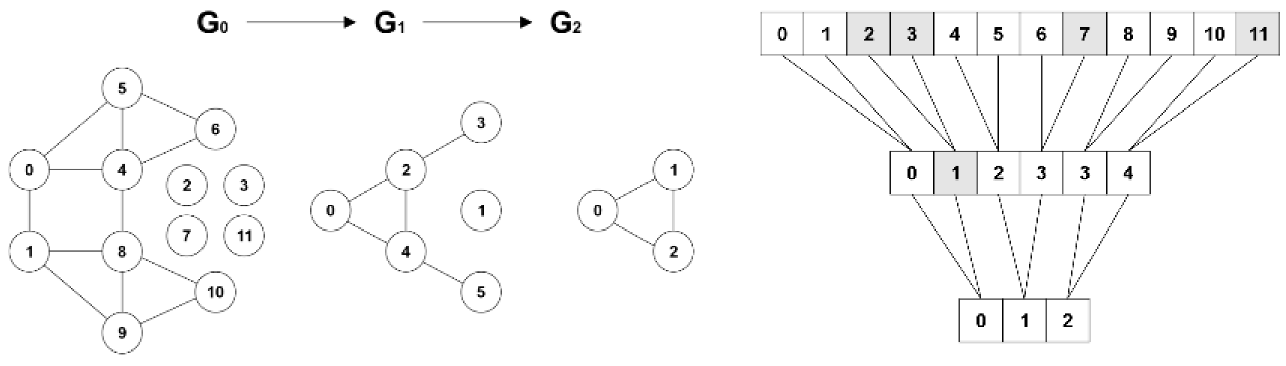

Figure 4 Example of Graph Coarsening and Pooling. [17]

All fake nodes added are initialized with neutral values, such as 0 if the network uses the Rectified Linear Unit (ReLU) as activation function and the max-pooling. The ReLU activation will not react in backpropagation if the feature value is 0, and the max-pooling will always filter the fake nodes off.

3.1.3. Pooling on 3D Surface Mesh

The multi-level graph coarsening algorithm can re-arrange the original graph, which can make the pooling operation very efficient. But our goal is to apply the Fully Convolutional Network [11] on 3D surface meshes with each triangular face has a label. Therefore, we must convert the surface mesh into a graph structure with each node represent a triangular face on the mesh. We also need to set up proper edge weights between two neighborhood faces. The edge weight should be significantly large if the two corresponding faces tend to cluster together, or significantly small otherwise. In surface mesh, two faces are considered similar if the two faces tend to fit in the same plane. In other words, two faces are considered similar if the dihedral angle between the two faces is close to $180°$. Therefore, we can define the edge weights $w(\alpha, \beta)$ between two neighborhood faces α and β as:

$$w(\alpha, \beta) = -\log\left(\frac{\theta}{\pi} + \epsilon\right)$$

Where θ is the angle between two face normal in radian

$$\theta = \arccos\{\vec{n}(\alpha) \cdot \vec{n}(\beta)\}$$

so that the dihedral angle $\omega = \pi - \theta$. The constant ϵ is the smallest float number to avoid log zero problems. And face normal should be three-dimensional unit vectors.

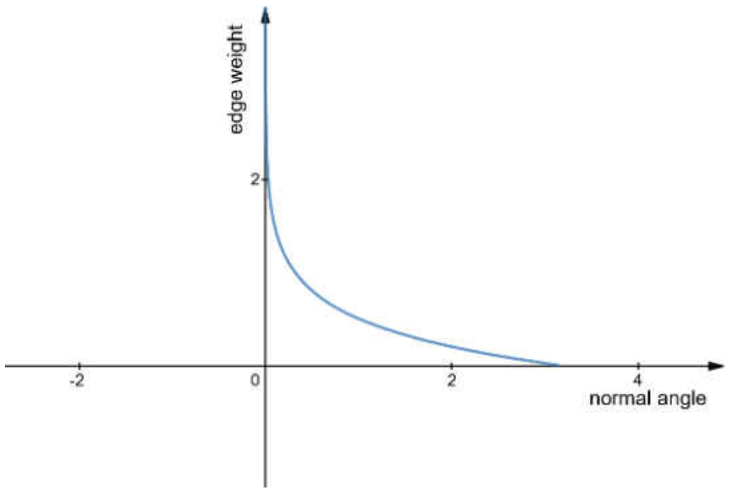

Figure 5 $w(\alpha, \beta)$ will be significantly large if θ is close to 0 (dihedral angle between the two faces is close to $180°$)

Now the original surface mesh, like figure 6 (b), can be represented by a graph $G(V, E, W)$, as shown in figure 6 (c), with vertices V represents all the triangular faces, edge E represents the neighborhood relationship, and edge weight W represents the tendency of clustering.

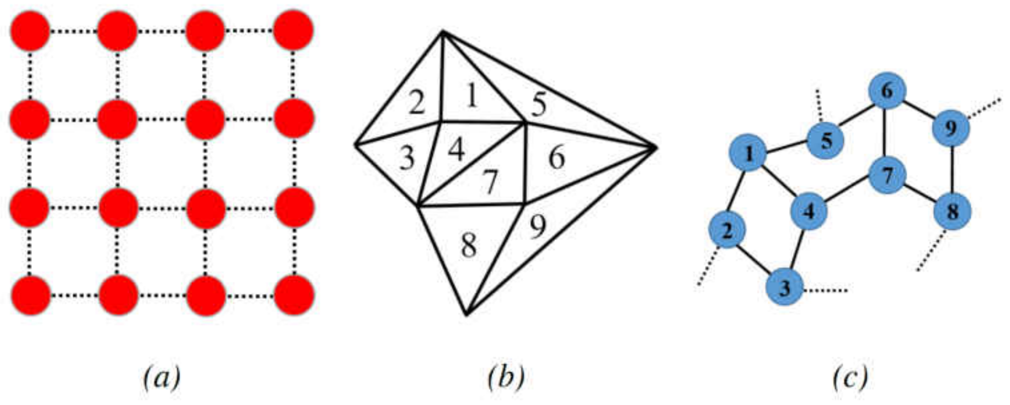

Figure 6 (a) Image data representation; (b) surface mesh representation; (c) surface mesh represented as graph structure [14]

The entire multi-level coarsening algorithm then can be described as a function that takes a graph G as an argument, the number of levels as a parameter and returns a list of coarsened graphs and a permutation vector which can permute the original faces vector for fast pooling:

$$coarsening(G, level = 10) \rightarrow ([G_0 \cdots G_m], perm)$$

If 5 pooling operation of size $(4, 1)$ is applied in the network, then 10 levels of coarsening are required because each level only reduces the number of nodes to half of its original amount.

3.2. Convolution Operation

The coarsening operation provides a way to permute the original graph into an order that pooling can be comfortably applied. However, the convolution operation requires a more structured neighborhood relationship and ordering. The graph built from a surface mesh has neighborhood relationships, just like an image. But the irregularity of the neighborhood structure restrains it from being directly represented and applied to the convolution operation. Therefore, restructuring the graph representation is necessary.

3.2.1. Generating Neighborhood

In order to re-construct the graph for convolution operation, each triangular face is viewed as a source node, and the breadth-first graph search is applied to generate a set of K nodes (a source node associated with $K-1$ neighbors), as shown in figure 7 (a) and (b). Then based on the generated neighborhood structure, like figure 6 (c), a convolution kernel of shape $(1, K)$ can be easily applied.

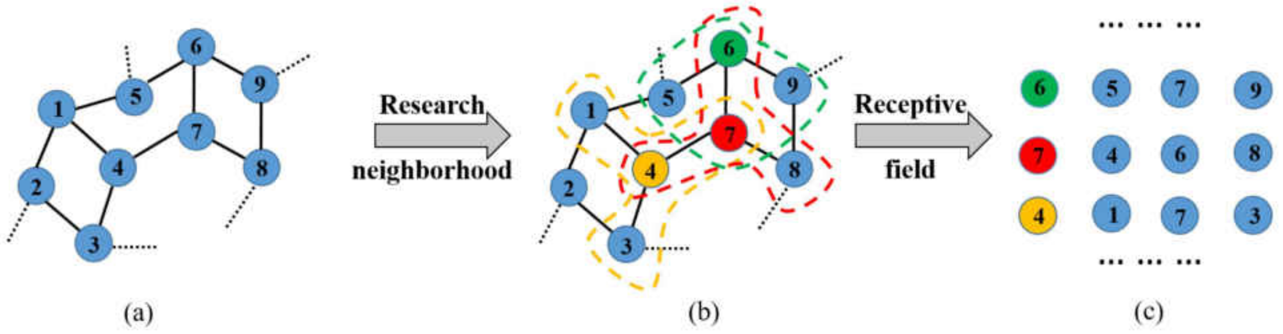

Figure 7 Convolution process on a shape [14]. (a) surface mesh represented as a graph; (b) the neighborhood nodes of different sources after breadth-first graph search; (c) convolution order of each neighborhood set.

Since a convolution operation is needed after each pooling, we have to determine the neighbors of the coarsened graph after each pooling stage. To achieve this, we need to apply a neighborhood search on each graph returned from the coarsening algorithm.

3.2.2. Convolution Order

Another problem when process convolution operation is the convolution order. When performing the convolution operation on an image, it is easy to determine the order of the convolution according to the spatial arrangement of the pixels. But it is rather challenging to determine the spatial orders amount the 3-dimensional surface mesh. Hence, sorting is applied after the neighborhood generation. Sorting ensures that the elements in each neighborhood set can be convolved by the same rules, so the convolution operation can better activate features. In this work, the neighbors are sorted based on the L2 similarity in the input feature space. Suppose an input data has a 4-dimensional shape as $(samples, faces, neighbors, features)$. In the neighborhood dimension, the first element is always the current source node. All elements after it are neighbors of the source node. The purpose is to keep the source node as the first element and sort all its neighbors based on the L2 similarity between the source node and the neighbor node.

$$L_2 = (neighbor[i] - neighbor[0])^2, \qquad i \in [1, num\ of\ neighbors]$$

If more than one feature is presented, then the summation of the L2 similarity for all features is used to sort the neighbors.

3.3. SFCN Architecture

After reconstructing the graph so that pooling and convolution operations can be easily applied, a Shape Fully Convolution Network then designed to process the segmentation task. First, reconstruct the data using the multi-level coarsening and breadth-first neighborhood searching algorithm. Then apply the Fully Convolutional Network [11] using convolution kernel of $(1, n + 1)$, pooling size of $(4, 1)$, and deconvolution kernel of $(4, 1)$ with stride $(4, 1)$. where n denotes the neighborhood size of each face.

3.3.1. Input Data

First, a graph $G(V, E, W)$ is created based on the face adjacency relationship of a surface mesh M. Where V is a set of faces on the mesh, E is a set of adjacent faces, and W is the set of weights calculated based on the dihedral angle between two adjacent faces. Then the multi-level coarsening algorithm is applied to the graph to get the pooling order. The algorithm will return a list of coarsened graphs and a permutation vector P which can re-organize the original data into an order that pooling can be easily applied.

$$([G_0 \cdots G_9], P) \leftarrow coarsening(G, level = 10)$$

The breath-first search algorithm is then applied to the coarsened graph G_i with $i \in even\ nuber$ to match the pooling size of 4.

$$[N_0 \cdots N_4] \leftarrow breath\_first\_search([G_0, G_2, G_4, G_6, G_8])$$

N_i should have the shape as (m_i, n) with m_i denotes the number of nodes in the graph G_i and n denotes the neighbor size. At the same time, the original input data with shape as (f, c) are permuted based on the permutation vector P in the first dimension. The result after permutation should have the shape as (h, c) where h represents the number of nodes of the base graph G_0 after adding all the fake notes. Finally, the permuted result is reshaped to 3-dimensional data with shape (h, 1, c) and use as input data to the network.

3.3.2. Generating Layer

The Shape Fully Convolutional Network [14] includes a generating layer before each convolution layer to process the convolution operation properly. First, as shown in Figure 8 (a), the input data are pre-permuted based on the permutation vector calculated from the multi-level coarsening algorithm. Second, the neighborhood indices, as shown in Figure 8 (b), are pre-calculated by the breadth-first graph search algorithm, and the neighbors are sorted based on the L2 similarity between the source node and each of its neighbor. Finally, the original data and the neighbors are concatenated together in the neighbor dimension makes the output has the shape as $(f, n+1, c)$, as shown in Figure 8 (c), where each row is sequenced in the convolution order represents a neighborhood set of $n+1$ nodes. By storing data in this way, we can achieve the convolution operation by row and pooling operation by column.

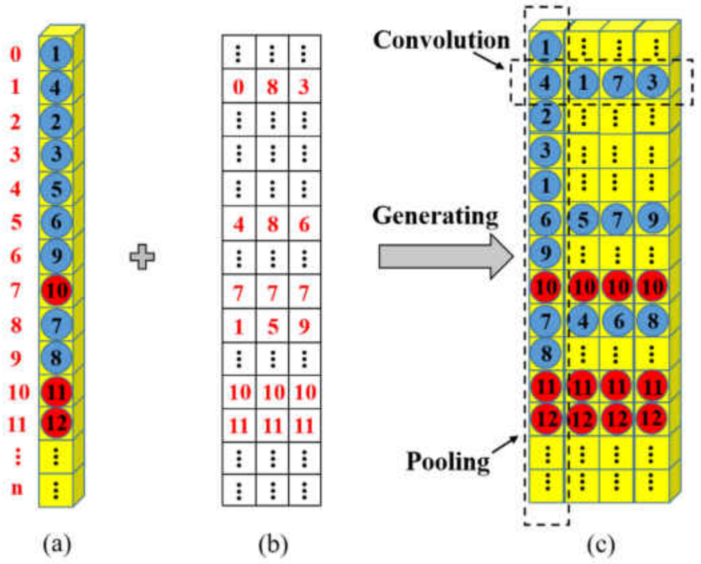

Figure 8 Generating Layer [14]. (a) the permutation vector, the nodes in blue represent true node on the graph, nodes in the red are fake nodes. (b) neighborhood set of each node, data represent the offset of each node. (c) outputs of the generating layer, where the convolution operation can be applied by row, and the pooling operation can be applied by column.

3.3.3. Convolution Layer

The name “convolution” indicates that the layer employs a mathematical operation called convolution. Convolution is a specialized kind of linear operation. In the implementation, instead of setup each unit inside a layer as a set of weights to all features of input data, we consider each unit as a filter (kernel), which has much fewer parameters but will be shared by all features. The convolution layer designed for the graph follows the same rule as to apply the convolution operation on 2D-images, which are shown in Figure 9.

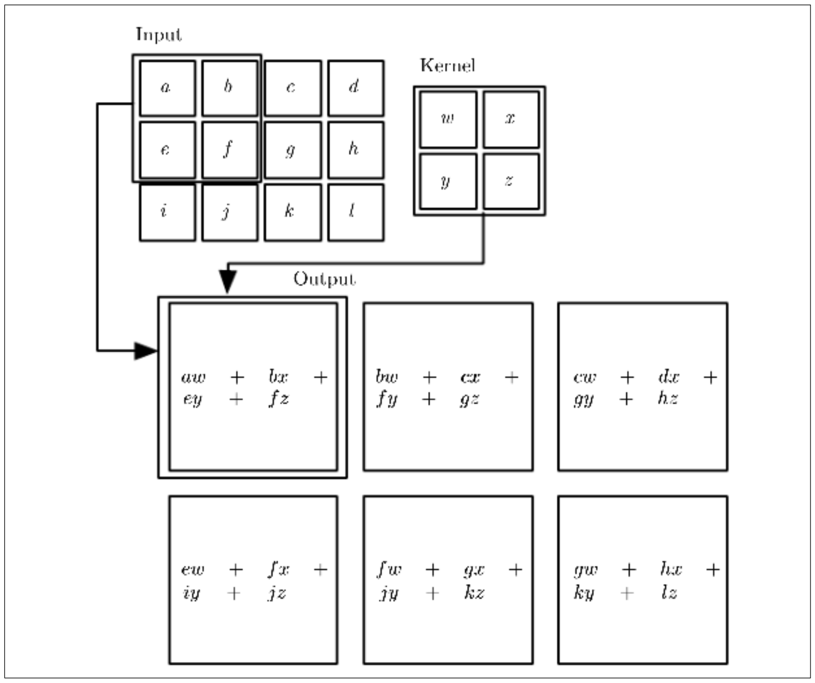

Figure 9 2-D Convolution Operation [4]

The output shape (H_{out}, W_{out}) can be calculated by the equations as follow:

$$H_{out} = \left\lfloor \frac{H_{in} + 2p_H - f_H}{s_H} + 1 \right\rfloor$$

$$W_{out} = \left\lfloor \frac{W_{in} + 2p_W - f_W}{s_W} + 1 \right\rfloor$$

Where (H_{in}, W_{in}) represent the shape of input to the convolution layer. p_H and p_W represent the vertical and horizontal padding. s_H and s_W represent the vertical and horizontal stride. And (f_H, f_W) is the shape of the filter.

As discussed in section 4.2.1, the generating layer will distribute the data into shape $(f, n+1, c)$. Then a convolution layer with $(1, n+1, c)$ is then applied to it. We use no padding $[(p_H, p_W) = (0, 0)]$ and single strides $[(s_H, s_W) = (1, 1)]$. Based on the equation, we can get the output shape as $(f, 1, c)$, as shown in Figure 10.

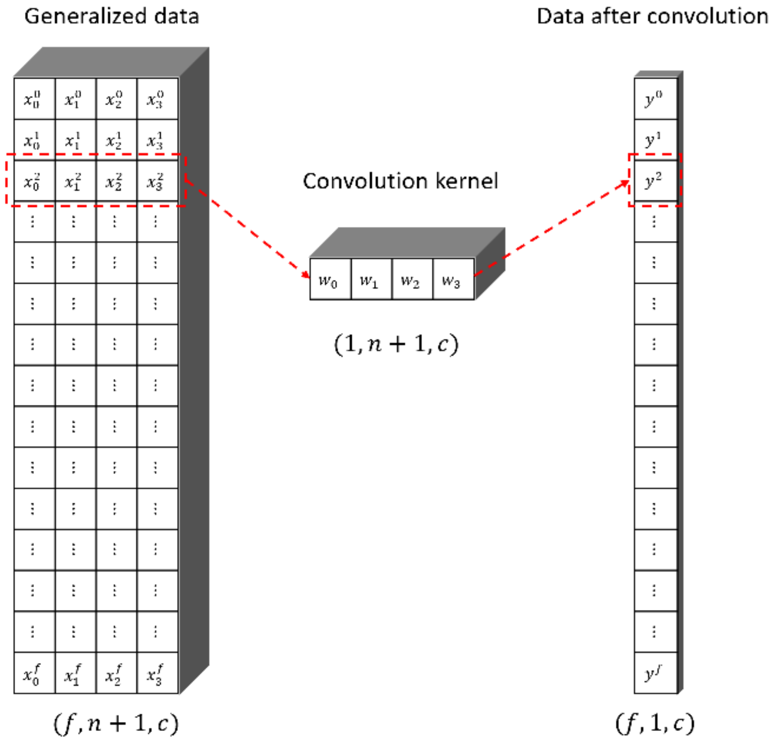

Figure 10 The convolution operation after generating layer, the subscriptions represent the neighbor dimension indices, and the superscriptions represent the face dimension indices.

3.3.4. Pooling Layer

A pooling layer is usually added after the convolution layer to reduce the size of the representation. At the same time, the pooling layer can kind of "highlight" the important information after convolution in case of speed up the calculation and make the feature detection more robust. In the Shape Fully Convolution Network, a max-pooling with shape $(4, 1)$ and stride $(4, 1)$ is applied after each convolution layer, which reduces the face dimension to a quarter of its original representation, as shown in Figure 11. Because all the fake nodes added have 0 as their features and all those zeros have no effect on the networks because of the Rectified Linear Unit (ReLU) activation. Therefore, by using max-pooling, the output will always be the most significant real nodes or fake node if all four of its original inputs are fake.

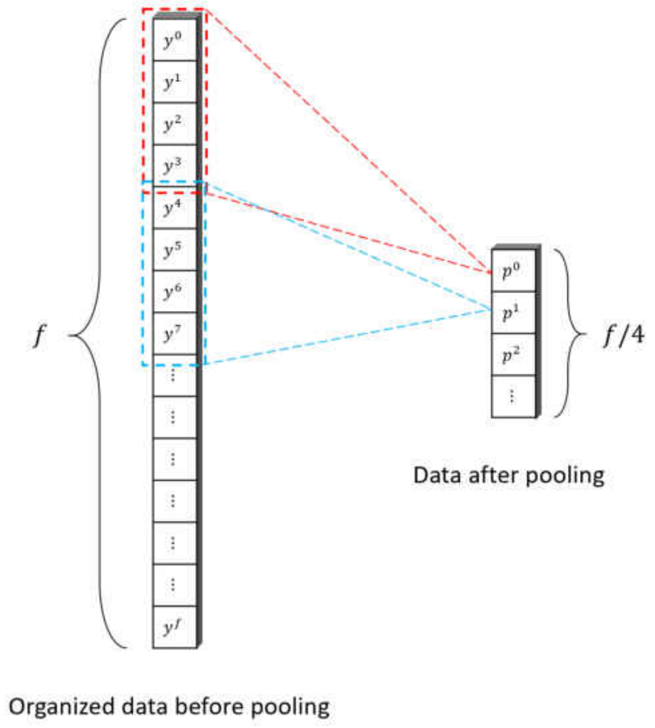

Figure 11 Pooling operation where $p^0 = max\ (y^0, y^1, y^2, y^3)$, $p^2 = max\ (y^4, y^5, y^6, y^7)$, *and etc.*

3.3.5. Deconvolution Layer

Like the Fully Convolutional Network [11], the Shape Fully Convolutional Network [14] architecture still needs the expansive path before the output layer to achieve the pixel-wise or triangular face wise prediction. There are several ways to process up-sampling. In the Fully Convolutional Network [11], a learnable up-sampling strategy named deconvolution operation or transpose convolution operation is applied to allow the network itself to figure out the optimal up-sampling through backward-propagation. The idea is the same as convolution operation but in an inversed way. Figure 12 shows the details of the deconvolution operation

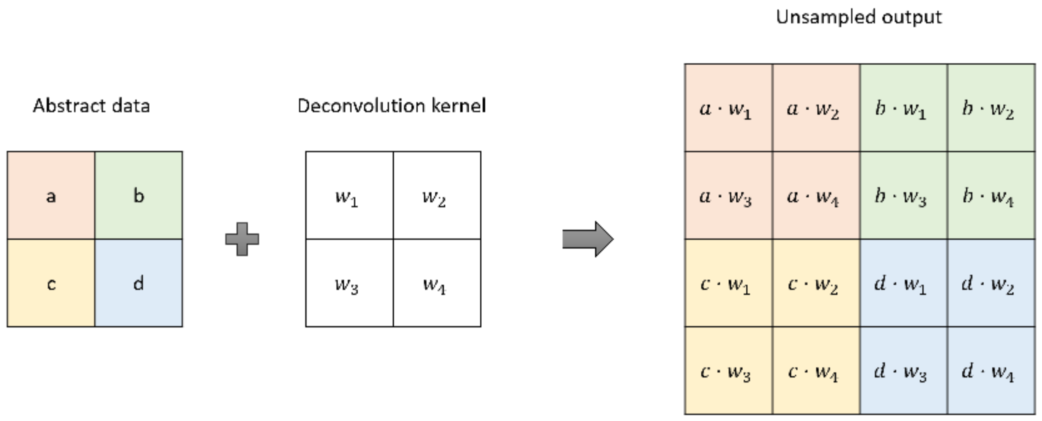

Figure 12 Image-based deconvolution operation with filter shape $(2, 2)$ *and stride* $(2, 2)$

In the Shape Fully Convolutional Network [14], the deconvolution layer can also be used to up-sample the data. As described previously, the SFCN regards pooling as a graph coarsening by clustering 4 vertices. Therefore, it is easy to reuse the image-based deconvolution implementation in the Fully Convolutional Network [11]. The difference is that the width of the deconvolutional kernel in the original FCN architecture is changed to 1, and the height and stride are set to the pooling size, which is 4. Figure 13 shows the details about the deconvolution operation in SFCN.

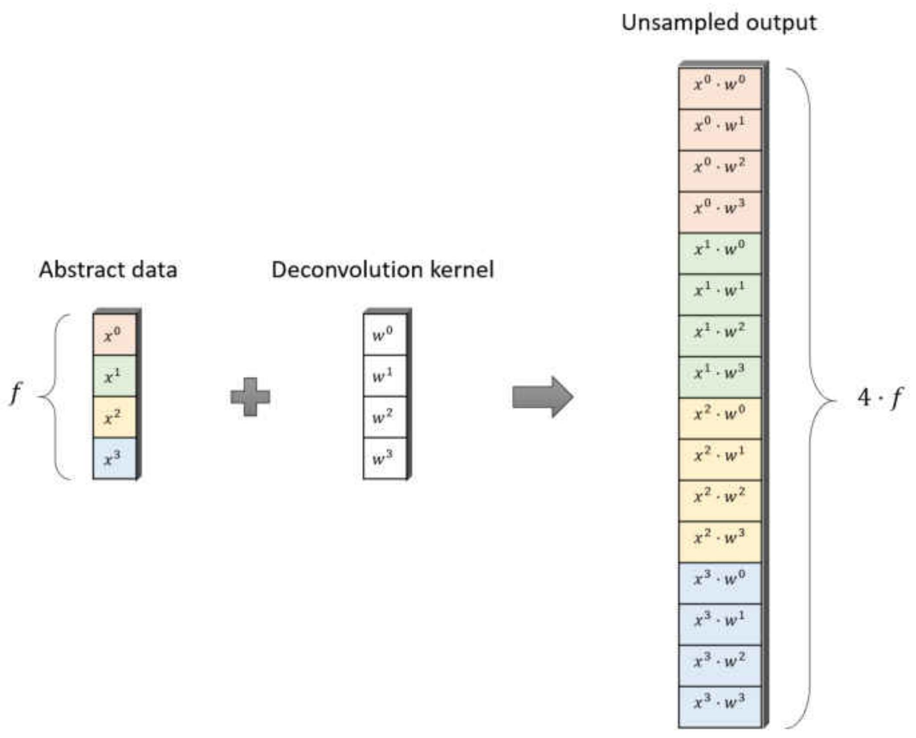

Figure 13 Deconvolution operation in SFCN with kernel size $(4, 1)$ *and stride* $(4, 1)$

3.3.6. The SFCN Architecture

The Shape Fully Convolutional Network [14] is an architecture that combines all the layers discussed above. Figure 14 shows the detailed SFCN structure with a single sample as input. It includes five stages in the down-sampling path and five stages in the up-sampling or expansive path. The input data should be a four-dimensional matrix with shape as $(s, f, 1, c)$, where s is the sample size, f is the number of faces per sample, the third dimension is the reserved neighborhood dimension which should be 1 as input, and c is the channel dimension or number of features. It then followed by the down-sampling path that includes five stages with each stage have a generating layer followed by a convolution layer, then followed by a max-pooling layer. Each generating layer takes two inputs: the original input or the output from previous pooling, and the neighbor indices. It will generate the neighborhood features based on the neighbor indices and concatenate them with the original input, or the pooling output in the neighborhood dimension, which makes the neighborhood size equals to $n + 1$, where n is the number of neighbors. After the generating layer, a 2-D convolution layer is applied to the generated data with kernel shape as $(1, n + 1)$, single stride, and no padding. Finally, at each stage, a max-pooling of shape $(4, 1)$ is attached after each convolution to high light the extracted features.

For the expansive or up-sampling path, five de-convolution layers are applied with each deconvolution kernel has the shape $(4, 1)$ and stride $(4, 1)$. Also, a skip is applied between the down-sampling path and the up-sampling path at each stage. The skip architecture [11, 35] will combine the coarse, high layer information with the fine, low layer information. Two fully convolution layers are used to connect the down-sampling path and the up-sampling path to learning the abstract features. Finally, a SoftMax layer is used as the output layer to predict a probability map for all possible labels of each triangular face.

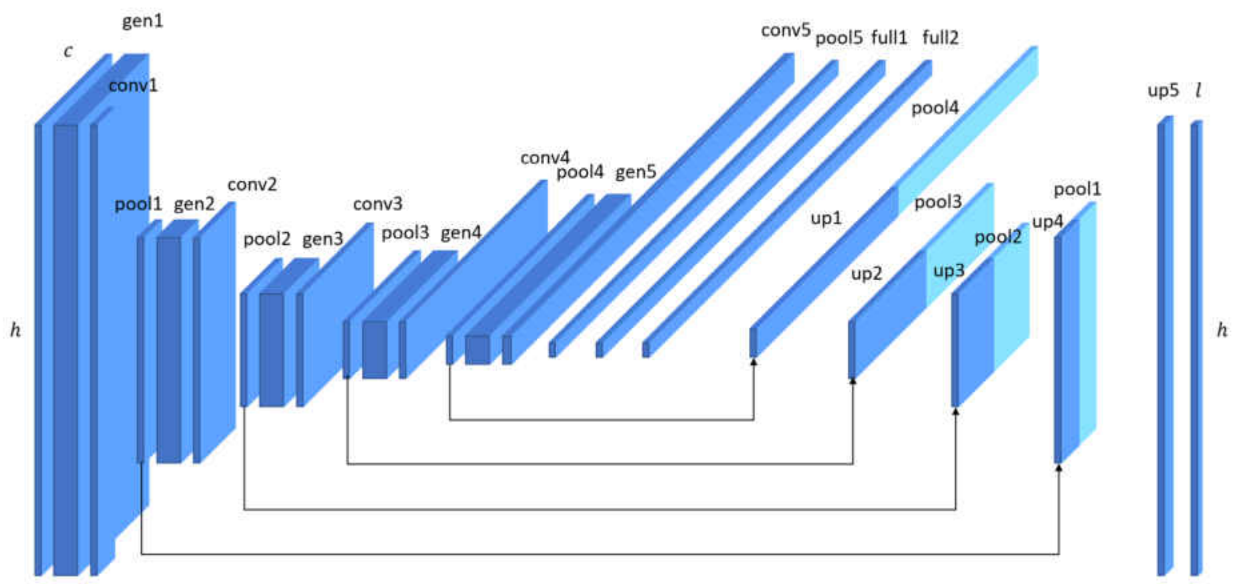

Figure 14 The SFCN Architecture for a single input sample

	gen1:(f,n,c)	*gen3:(f/16,n,128)*	*gen5:(f/256,n,512)*	*[up2,pool3]:(f/64,1,512)*	
	conv1:(f,1,64)	*conv3:(f/16,1,256),*	*conv5:(f/256,1,1024)*	*[up3,pool2]:(f/16,1,256)*	
input:(f,1,c)	*pool1:(f/4,1,64)*	*pool3:(f/64,1,256)*	*pool5:(f/1024,1,1024)*	*[up4,pool1]:(f/4,1,128)*	*out:(f,1, l)*
	gen2:(f/4,n64)	*gen4:(f/64,n,256)*	*full1:(f/1024,1,1024)*	*up5:(f,1,32)*	
	conv2:(f/4,1,128)	*conv4:(f/64,1,512)*	*full2:(f/1024,1,1024)*		
	pool2:(f/16,1,128)	*pool4:(f/256,1,512)*	*[up1,pool4]:(f/256,1,1024)*		

4. Features on 3D Polygon Mesh

In the colored 2D image, the features are the RGB data of each pixel. All the colors are globally well defined so that each specific color is mapped to the same RGB value though out all colored images. Therefore, it is safe to directly use the raw RGB data and let the network itself to figure out the abstract features. However, it is not the case when using 3D polygon mesh as input data. The raw data used to form a 3D polygon mesh usually include the local $[x, y, z]$ coordinates of each vertex and the vertex indices of each triangular face. Some times the face normal of each face is also recorded. All these pieces of information are defined locally, which means the same object may have different coordinates or different surface normals if it is put in different files with different orientations or different sizes, or if the object is simplified or re-meshed. Hanse, it is not practical to feed the network directly with the raw information of the surface mesh.

The features we use to feed the Shape Fully Convolution Network should have two properties:

- They should be defined for each triangular face since we treat each face as a node of the graph
- The features should independent with the transformation, rotation, simplification, and subdivision so that the same object should have relatively the same features with different sizes or different orientations.

There are a lot of features that can be defined to each triangular face and also independent with the orientation and the size, such as curvature [36], shape diameter function [37], distance from medial surface [38], average geodesic distance [39], shape context [40], and spin image [41]. In this implementation, the average geodesic distance

[39], the shape context [40], and the spin image [41] are pre-calculated and combined together as the triangular face wise features to feed the network.

4.1. Geodesic Distance

Geodesic, in definition, is equivalent to the absolute straight line on a curved surface. Geodesic distance is the distance of the straight line on the curved surface between two specific points. Based on the definition, the geodesic distance doesn't seem necessary to be the shortest path between those two points. However, consider the trade-off between computation cost and accuracy, on a polygon mesh, the shortest path between two points is a good approximation of the geodesic distance between those two points. Therefore, the finer the surface mesh is, the better the approximation can be. It is practical to limit the edge length to be smaller than a threshold.

In the implementation, for each vertex on the mesh, we calculate the shortest path to all other vertices using Dijkstra's algorithm. This function will return a matrix with shape as (v, v) where v represents the number of vertices in the mesh. And each value inside the matrix represents the shortest path from the row index vertex to the column index vertex.

$$vertex\_geodesic(mesh) \rightarrow matrix[v, v]$$

Then, the average geodesic distance is calculated to each vertex by averaging one dimension of the matrix. Finally, the average geodesic distance of each triangular face is approximated by averaging the vertex geodesic distance for three of its vertices. Figure 15 shows the face average geodesic distance on two objects from two different perspectives. We can see that the AGD value is small if close to the center of the object and large if close to the edge. Using the average geodesic distance provides rotation invariance shape descriptor. Normalize the average geodesic distance for each surface mesh to between $[0, 1]$ can make it also translation invariant.

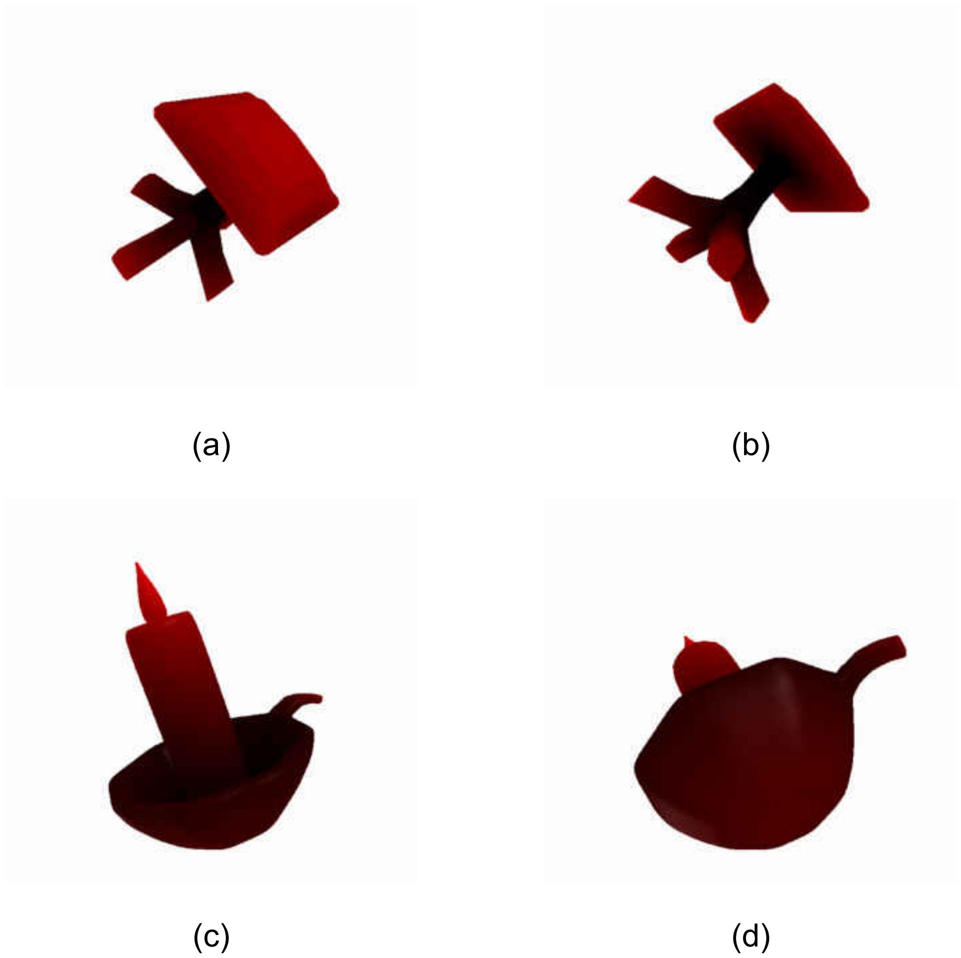

Figure 15 Examples of the distribution of the average geodesic distance, (a), (b) two perspectives of a chair, (c), (d) two perspectives of a candelabra

4.2. Shape Context

The shape context is originally proposed in a 2D shape matching algorithm in 2002 with each object as a point set [40]. To see whether two shapes can be matched with each other, some kinds of shape descriptor is needed for the comparison. The initial idea is to use the vector originating from a point to all other sample points on the shape as a descriptor. Obviously, this will form a matrix with the shape of $(n, n-1)$, where n represent the number of points on the shape. However, since n gets larger, this full set of vectors is much too detailed, and most importantly, consume too much processing power when using it. The concept of shape context comes above this idea. They propose that the distribution over relative positions of each point is a more robust and compact, yet highly discriminative descriptor.

The shape context is formed as follow: for a point p_i on the shape, compute a coarse histogram h_i of the relative coordinates of the remaining $n-1$ points, where the bins of the histogram are uniform in log-polar[2] space, which makes the descriptor more sensitive to positions of nearby sample points than to those of points farther away. Figure 16 shows an example.

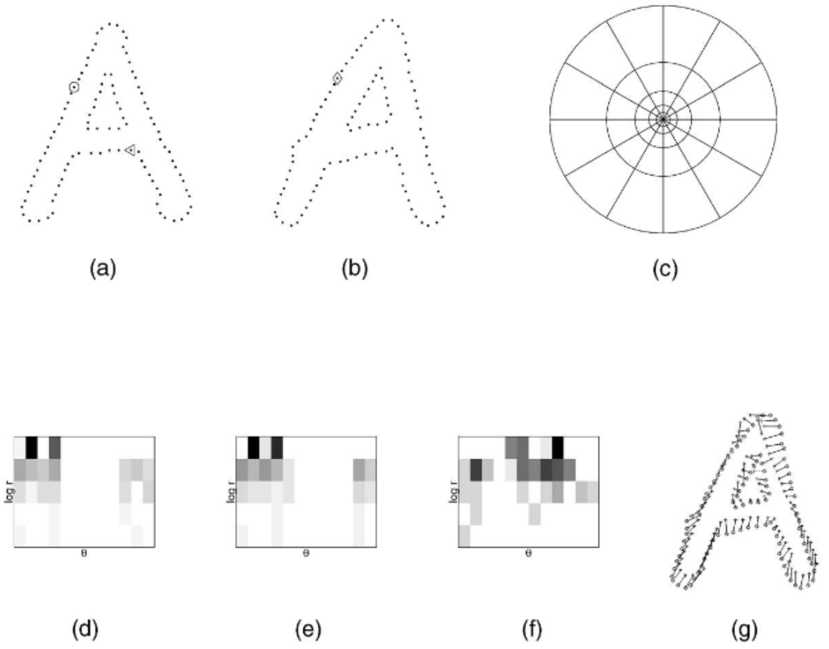

Figure 16 Shape context computation and matching [40]. (a) and (b) Sampled points. (c) log-polar bins with five bins for $log(r)$ and 12 bins for θ. (d), (e), (f) Shape context of three points marked as ○ ◁ ◇.(g) correspondences found using bipartite matching

The similar concept of shape context is applied to 3D triangular meshes with some variance. The geodesic distances from a triangular face to all other vertices are approximated as described in section 5.1, and 5 logarithmic geodesic distance bins are used. On the other side, 6 uniform angle bins are formed, where angles are measured relative to the normal of each face. This will form a 5 by 6 histogram yielding 30 features total. Figure 17 and Figure 18 show two examples of shape context formed from two faces on two different shapes.

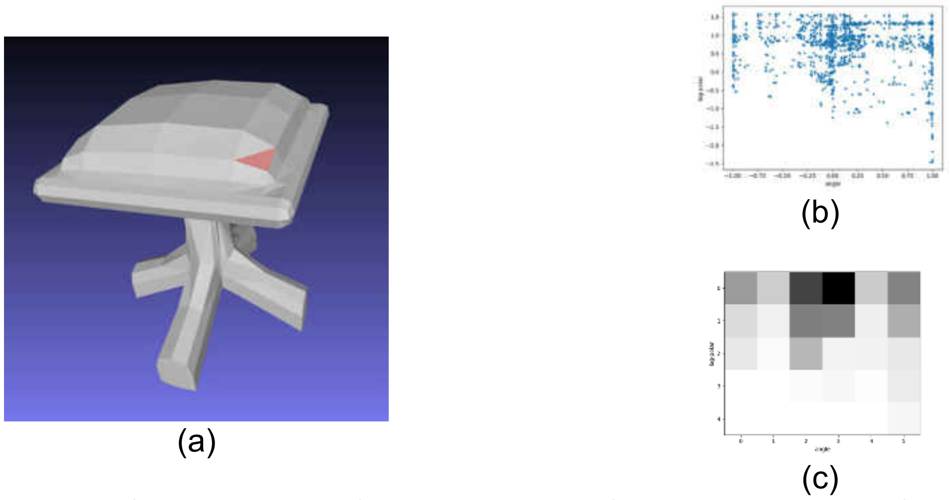

Figure 17 Example of a shape context (a) face select on a mesh of chair, (b) the distribution of all other vertices in $log(r)$ and angle space, (c) the shape context with 5 $log\ (r)$ bins and 6 angle bins.

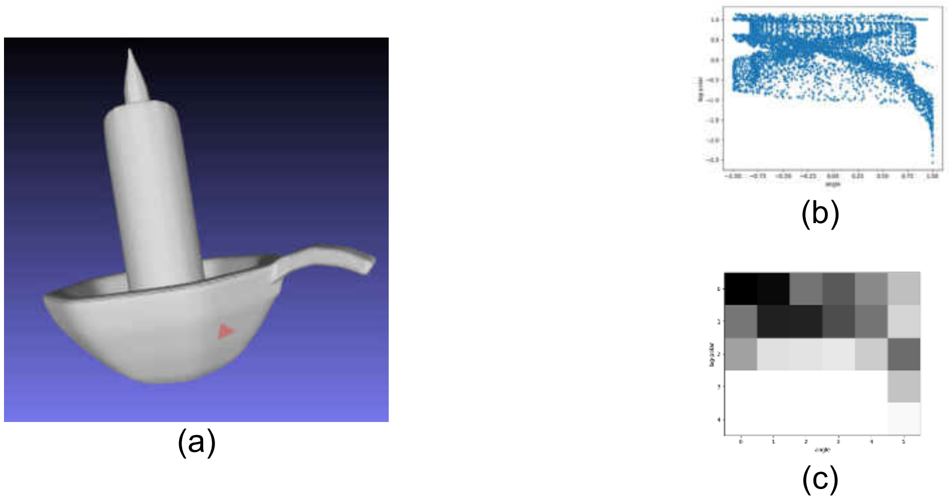

Figure 18 Example of a shape context (a) face select on a mesh of candelabra, (b) the distribution of all other vertices in $log(r)$ and angle space, (c) the shape context with 5 $log\ (r)$ bins and 6 angle bins.

4.3. Spin Image

Spin image is another shape descriptor for shape matching, which is proposed by Andrew E. Johnson in 1999 [41]. The original idea is based on the oriented point cloud object representation, where each point on the object has a surface normal as its direction. If the object representation is a polygon mesh, then the surface normal at a vertex is computed by fitting a plane to the points connected with this vertex. An oriented point can form a partial, object-centered, coordinate system. Two cylindrical coordinates α and β are defined respect to the oriented point. α defined as the perpendicular distance to the line of the surface normal. Since this is the distance from a point to a line, the value should always be positive. β defined as the signed perpendicular distance to the tangent plane defined by vertex normal and position. This is the distance from a point to a plane. Since the point can be either above or below the plane. The value of β could be either positive or negative. Figure 19 shows an example of an oriented point basis created at a vertex in a surface mesh.

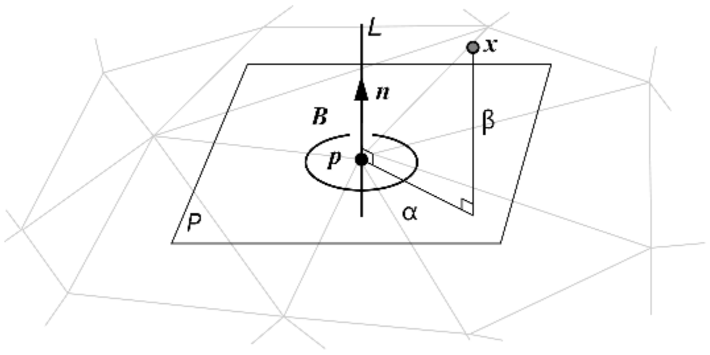

Figure 19 An oriented point basis created at a vertex in a surface mesh [41]

β can be calculated by first computing the vector from the origin point to each other vertices, then process the dot product between this vector and the surface normal.

$$\beta = \vec{n} \cdot \overrightarrow{(x-p)}$$

where x and p are 3D coordinates of the vertex, and $\vec{n}$ is the surface normal unit vector. Since the surface normal is a unit vector, the dot product of the two vectors will return the projection of the $\overrightarrow{(x-p)}$ vector on $\vec{n}$ direction, where if x is above the plane, the projection is positive, otherwise negative. After computing β, then α can be obtained by:

$$\alpha = \sqrt{\left\|\overrightarrow{(x-p)}\right\|^2 - \beta^2}$$

After (α, β) coordinates are computed for each vertex on the surface mesh. The bins indexed by (α, β) are then created as accumulators to recode the histogram about how many points are laid on each bin. Figure 20 shows an example of three spin images generated from three different oriented points.

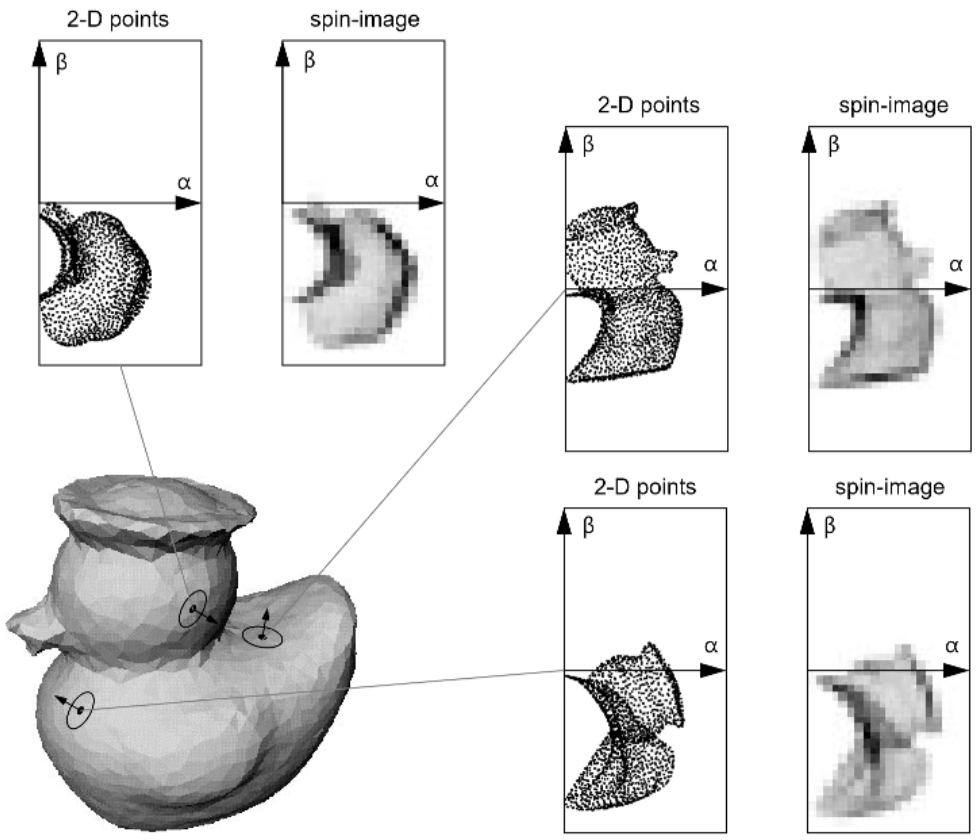

Figure 20 Spin images for three different oriented points on a surface mesh [41]

There are three important parameters to generate the spin image: bin size, image width, and support angle. The bin size is simply the size of each bin on α and β axis; in another word, it decides the boundary condition of which bin should a vertex be projected to. figure 21 shows an example of different spin images on different bin sizes.

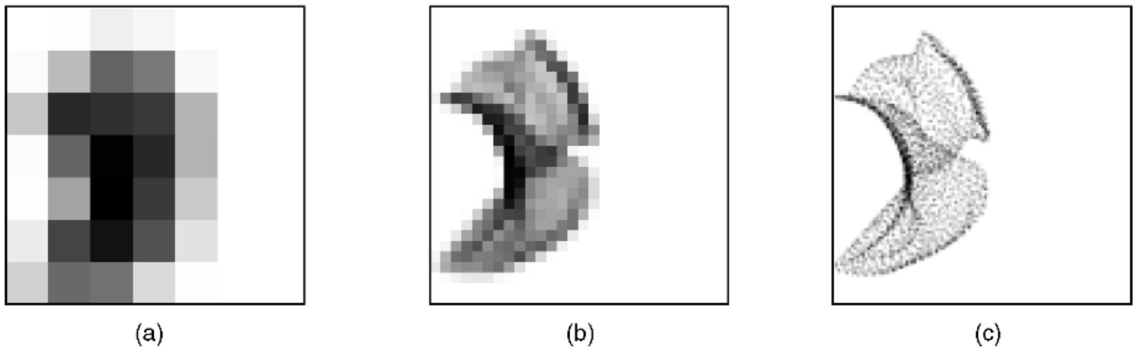

Figure 21 The effect of bin size on the spin image [41] (a) 4x mesh resolution, (b) 1x mesh resolution, (c) 1/4x mesh resolution

In practical, this parameter is set to the mesh resolution, which is the median edge length across the entire surface mesh.

The next parameter is the image width, which determines the output size of a spin image. Although spin images can have any number of rows and columns, for simplicity, a squared image with equal height and width is usually used. Then the equation relating spin-map coordinates (α, β) and the spin image bin (i, j) are:

$$i = \left\lfloor \frac{\frac{W}{2} - \beta}{b} \right\rfloor \qquad j = \left\lfloor \frac{\alpha}{b} \right\rfloor$$

Where W is the image width and b is the bin size. Figure 22 shows an example of three different spin images from different image width.

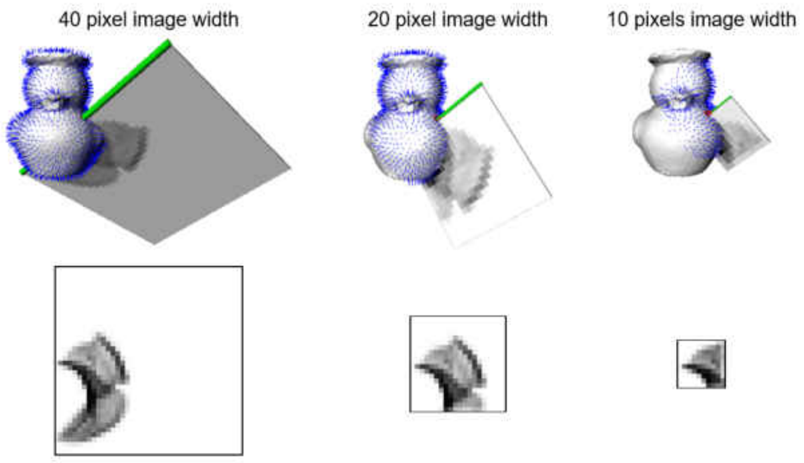

Figure 22 The effect of image width on the spin image [41]

The last parameter of generating the spin image is the support angle. It is the maximum angle between the direction of the oriented point of the spin image and the surface normal of other points. Suppose we have the origin point A with position and normal as $(p_A, \vec{n}_A)$, and another vertex B with position and normal as $(p_B, \vec{n}_B)$. Then the constraint of support angle ϕ_S is:

$$\mathrm{acos}(\vec{n}_A \cdot \vec{n}_B) < \phi_S$$

Figure 23 shows an example of three spin images generated from three different support angles

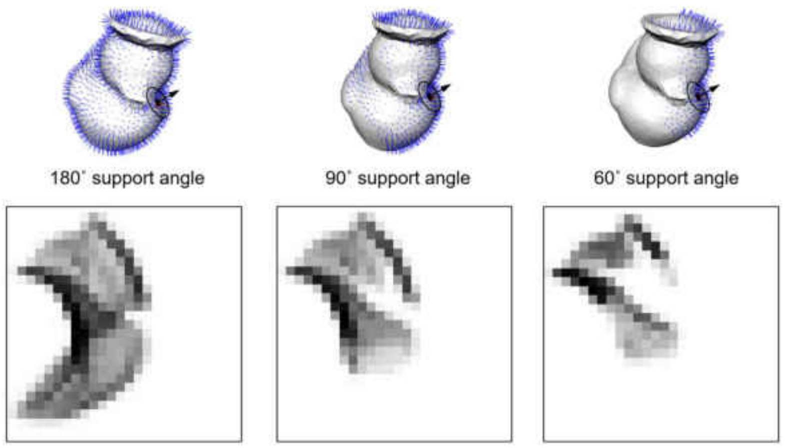

Figure 23 The effect of support angle on the spin image [41]

In our case, the spin images should be assigned to each triangular face instead of a vertex. Therefore, the center point of the face is used as the origin point position, and the surface normal of the triangular face is used as the oriented direction. Then the set of α is the distance from other vertices to the current surface normal. And the set of β is the distance from all other vertices to the current surface plane.

Originally, the spin image is designed for shape matching, which means they are looking for two .meshes with the same shape. Use a fixed image width associated with a bin size that is related to the mesh resolution, which is the median edge length of the mesh, makes the output spin image independent form the size of the shape. However, in our case, we are not only looking for the features that are size invariance, but they should also be invariant from transformations, such as re-meshing. Also,the meshes we used to train a network has many different shapes. So instead of using fixed bin size, we uniformly divide the α and β axis into 8 bins and always yielding 64 features for each triangular face. Figures 24 and 25 show two examples of how spin images are generated from a specific triangular face on different surface meshes.

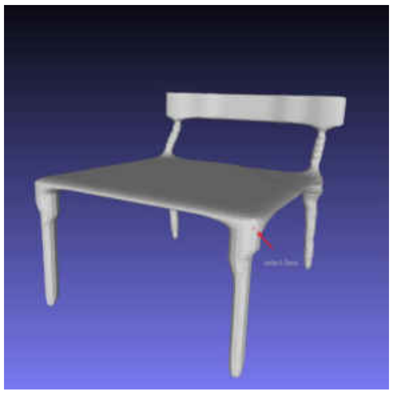
(a)

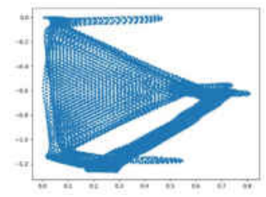
(b)

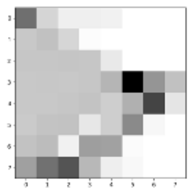
(c)

Figure 24 Example of a spin image (a) a face select on a mesh of chair, (b) the distribution of all other vertices in (α, β) coordinates, (c) the spin image with 8 uniform bins on both axis.

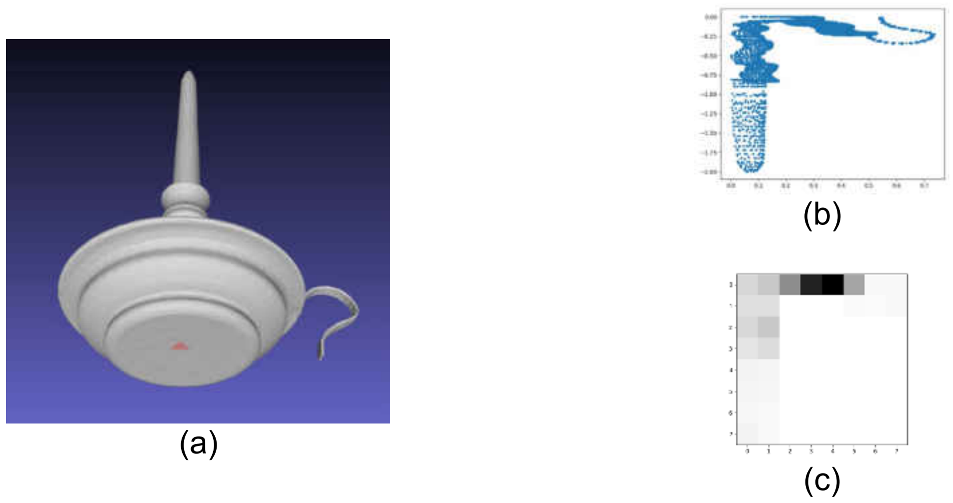

Figure 25 Example of a spin image (a) a face select on a mesh of candelabra, (b) the distribution of all other vertices in (α, β) coordinates, (c) the spin image with 8 uniform bins on both axis.

5. Post Optimization

After training, the network should be able to output a probability map that is able to assign labels to each face. However, inconsistency may arise among adjacent triangles, leading to unsatisfactory visual effects. A comment constraint is that the labels should be very smoothly almost everywhere while preserving sharp discontinuities that may exist. And this task is naturally formulated in terms of energy minimization. That is, to find a labeling l that minimizes the energy function

$$E(l) = E_{data}(l) + E_{smooth}(l)$$

E_{data} measures the disagreement between the labeling l and the observed data, or in another word, it evaluates a classifier:

$$E_{data}(l) = \sum_{p \in P} D_p(l_p)$$

Where D_p measures how well label l_p fits target p given the observed data. In SFCN [14], D_p is the predicted probability map, and the negative logarithm of $D_p$is used as the data term [14] [42].

$$E_{data} = -\log (D_p)$$

E_{smooth} measures the extent to which l is not piecewise smooth. It is a term that penalizes neighbors assigned different labels. In SFCN [14], they propose to compute the product of the dihedral angle and the side length between the adjacent faces. And serve it with a negative logarithm as the smooth term.

$$E_{smooth}(l_u, l_v) = \begin{cases} 0, & if\ l_u = l_v \\ -\log\left(\frac{\theta_{uv}}{\pi}\right) e_{uv}, & otherwise \end{cases}$$

Where θ_{uv} is the dihedral angle in degrees between face u and v, and e_{uv} is the distance between face u and v.

The NP-hardness of minimizing the energy function [32] effectively forces us to find an approximate solution. One way is to convert the problem into a graph and approximate the solution using a minimum graph cut algorithm [32]. The algorithm generates a labeling that is a local minimum of the energy in a $\alpha - \beta - swap$ move.

5.1. Finding the Optimal Swap Move

The $\alpha - \beta - swap$ algorithm [32] is described as follow: Given an input labeling f and pair of labels (α, β), we wish to find a labeling $\hat{f}$ that minimizes the energy over all labeling within one $\alpha - \beta$ swap:

```
1. Start with an arbitrary labeling $f$
2. Set success := 0
3. For each pair of labels $\{\alpha, \beta\} \subset \mathcal{L}$
   3.1. Find $\hat{f} = \arg\min E(f')$ among $f'$ within one $\alpha$-$\beta$ swap of $f$
   3.2. If $E(\hat{f}) < E(f)$, set $f$ := $\hat{f}$ and success := 1
4. If success = 1 goto 2
5. Return $f$
```

Figure 26 $\alpha - \beta - swap$ algorithm [32]

The algorithm is based on computing a labeling corresponding to a minimum cut on a graph $G_{\alpha\beta} = (V_{\alpha\beta}, E_{\alpha\beta})$. To build the graph $G_{\alpha\beta}$, we first need to generate an original graph based on the neighborhood relationship of the original data and the labeling α, β. Use the surface mesh as an example, all faces are labeled as α or β are treated as vertices $V_{\alpha\beta}$, and the neighborhood relationships across all these faces are treated as edges. These edges are called n-links or neighbor-links. Then, the graph $G_{\alpha\beta}$ is generated by adding two labeling α and β to the original graph as two vertices and connect each of these two vertices to all other vertices $v \in V_{\alpha\beta}$. In this graph, α and β are called two terminals, and the edges connect between terminals and other vertices are called t-links or terminal-links. Figure 27 shows an example of $G_{\alpha\beta}$.

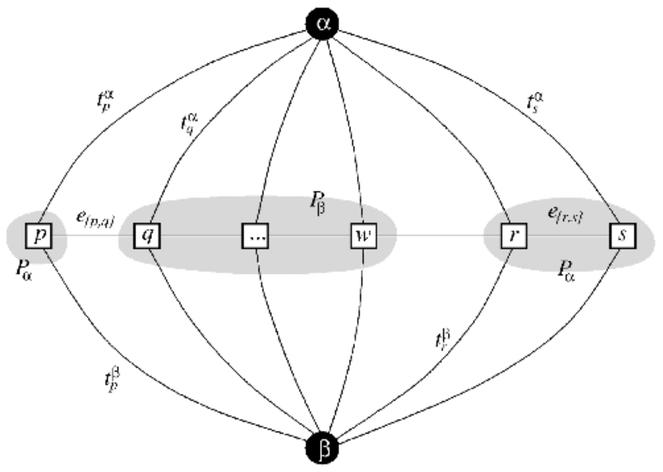

Figure 27 An example of the graph $G_{\alpha\beta}$ [32].

After generating the graph, weights are assigned to each edge as follow:

Edge	Weight
t_v^α	$E_{data}(\alpha) + \sum_{u \in N_v} E_{smooth}(v,u)$
t_v^β	$E_{data}(\beta) + \sum_{u \in N_v} E_{smooth}(v,u)$
$e(v,u)$	$E_{smooth}(v,u)$

Table 1 Weight for each edge in $G_{\alpha\beta}$ for $v \in V_{\alpha\beta}$, where N_v denotes the neighbor set of vertex v [32]

Based on the graph $G_{\alpha\beta}$, we try to find a minimum graph cut C, which must serve exactly one t-link for any vertices $v \in V_{\alpha\beta}$. In other words, the cut C should leave each vertex $v \in V_{\alpha\beta}$ with exactly one t-link, as shown in Figure 28. This defines a labeling f^C corresponding to a cut C on graph $G_{\alpha\beta}$:

$$f_v^C = \begin{cases} \alpha & if\ t_v^\alpha \in C \\ \beta & if\ t_v^\beta \in C \\ f_v & if\ v \notin V_{\alpha\beta} \end{cases}$$

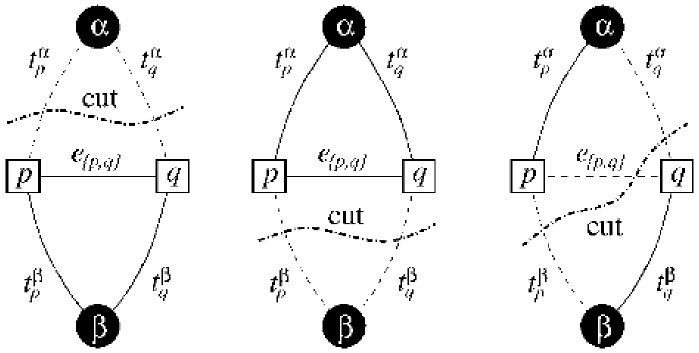

Figure 28 Properties of a cut C on graph $G_{\alpha\beta}$ for two neighbor vertices p, q [32]

In other words, $v \in V_{\alpha\beta}$ is assigned to label α if the cut C separates v from the terminal α; similarly, v is assigned to label β if the cut C separates v from the terminal β. If $v \notin V_{\alpha\beta}$, then keep the original label f_v.

6. Experiment Result

6.1. Data

The data used in this project are two existing large datasets from the Shape COSEG datasets [43], including the chair dataset of 400 shapes, and the vase dataset of 300 shapes.

6.2. Shape Fully Convolution Network Parameters

The network is trained by using Adam optimizer with a learning rate of 0.001, β_1 as 0.9 and β_2 as 0.999. The rectified linear unit (ReLU) is used as the activation function for all convolution and transposed convolution layers. A dropout layer of 40% is added between two (1×1) fully convolution layers at the finest level. Finally, the per-triangle prediction is achieved by a (1×1) fully convolution output layer with SoftMax as the activation function. The categorical cross-entropy loss function is used to minimize the cost.

6.3. Computation Time

The model is trained on a server with one Intel(R) Core(TM) i5-9400F CPU @ 2.90GHz with 6 cores and one NVIDIA GeForce RTX 2080 Ti GPU. On large datasets such as the Chairs dataset, 300 samples are used for training, and the training time for a single epoch is approximately 979 seconds, which yields to about 3 seconds per sample. However, if the sorting is removed from the generating layer, the training time will be reduced to approximately 8 seconds per epoch. In other words, the majority time spent on training is to sort all neighbors by their L2 similarity during the generating process. It is because the GPU is designed only for arithmetic computing, where the sorting is a comparison-based algorithm.

6.4. Result

6.4.1. Chairs Dataset

In this experiment, the model is trained separately by two datasets. For the Chairs dataset, 300 random samples are used for training, 50 samples are used for validation, and 50 samples are used for testing. The test accuracy is about 89%. However, the variation for the prediction is quite high. Figure 29 shows the accuracy plot for 50 samples in the test set.

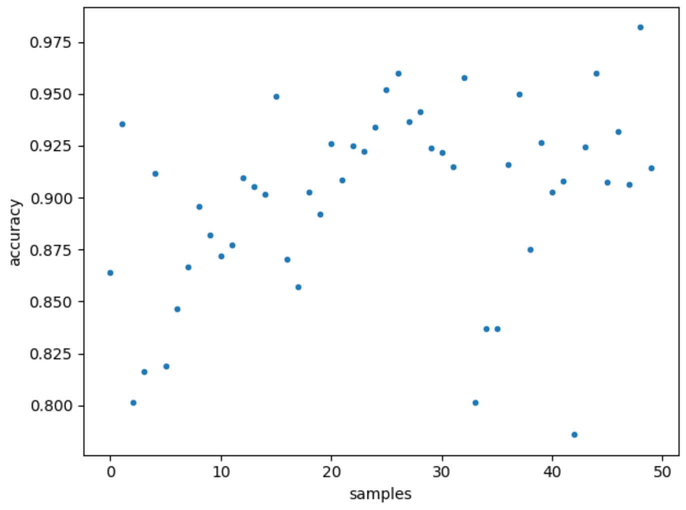

Figure 29 Accuracy plot for 50 test samples in the Chairs dataset

We can see that one sample has about 98% accuracy, and another has only about 78%.

After prediction, the optimization algorithm explained in section 5 is applied. The algorithm can optimize the labeling by providing punishment to the predicted result based on the smoothness of the surface, which suppose to be able to sharpen the edges between two labels. But based on the experiment result on this data set, the optimization algorithm doesn't improve accuracy significantly. Table 2 shows the visualization of three samples from the test set.

Ground Truth	Prediction	accuracy	Optimization	accuracy
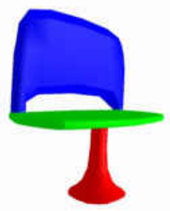	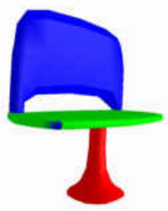	91.83%	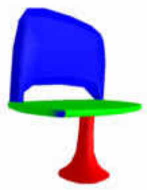	91.92%
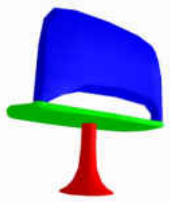	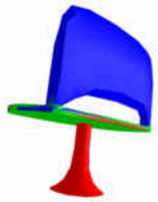		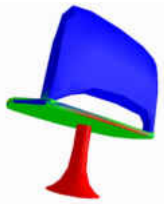	
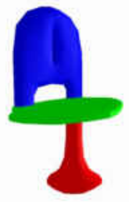	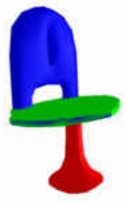	93.21%	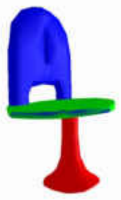	93.12%
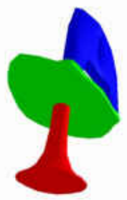	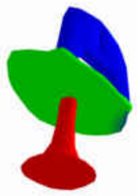		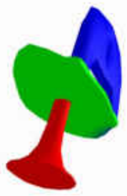	
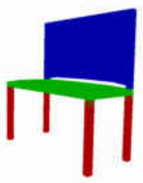	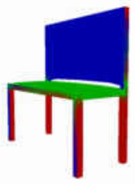	80.07%	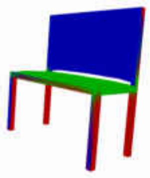	80.15%
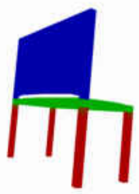	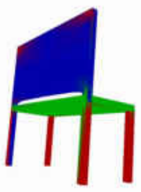		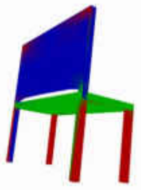	

Table 2 Visualization of Three samples from the Chairs test set

6.4.2. Vases Dataset

The vases dataset has 300 samples. Because of the sample size of this data set is relatively small than the Chairs data set. Instead of using a similar rate for training, validation, and testing as the Chairs dataset. I use 250 for training and 50 samples for testing. The accuracy of the test set is about 83.5% on average. The same with the Chair dataset, the varication of the testing accuracy is also high. Figure 30 shows the accuracy plot for 50 testing data:

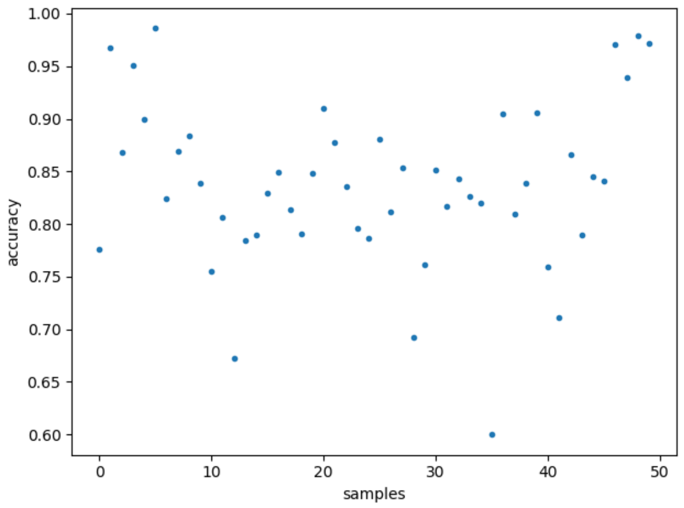

Figure 30 Accuracy plot for 50 test samples in the Vases dataset

Obviously, there are a couple of samples have accuracy above 95%, and some others below 70%. The lowest prediction accuracy is 60% for this data set.

The same with the Chairs data set, the multi-label graph cut algorithm is applied to the predicted labels to optimize the result. Table 3 shows the visualization of three samples from the dataset. The result shows that the model is able to separate between the base, the neck, and the body of a vase but not very well for the handles. Also, the post-optimization doesn’t provide significant improvement to the final result.

Ground Truth	Prediction	accuracy	Optimization	accuracy
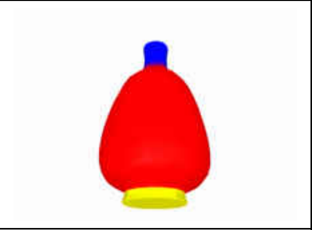	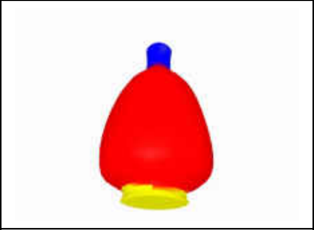	98.62%	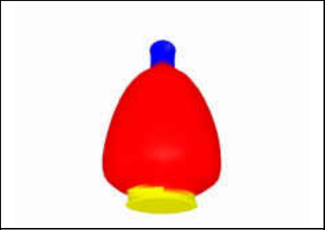	98.62%
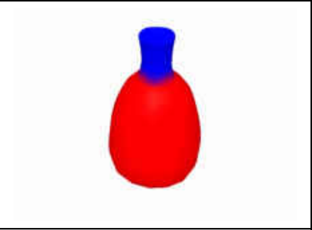	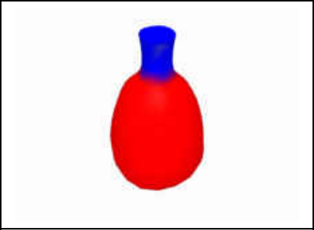		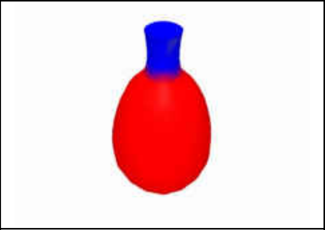	
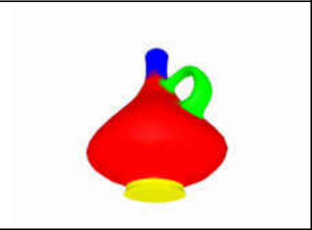	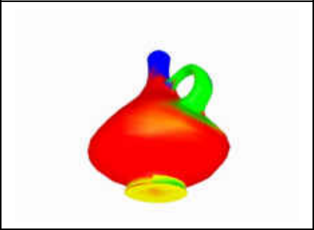	86.90%	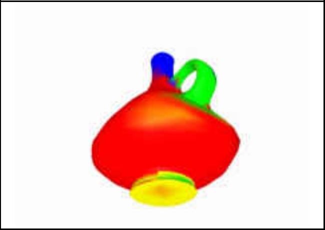	86.93%
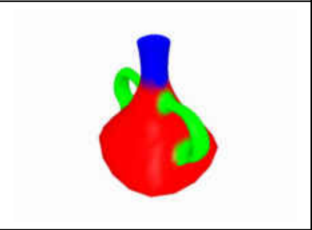	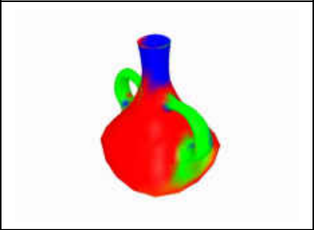		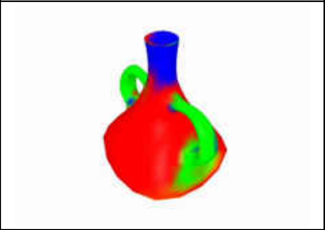	
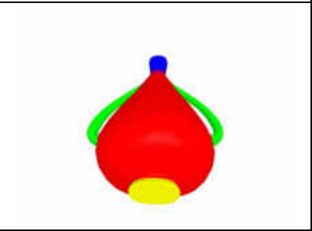	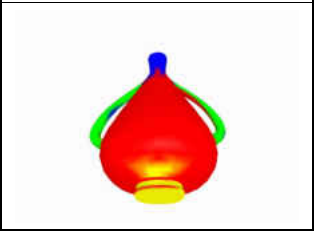	83.89%	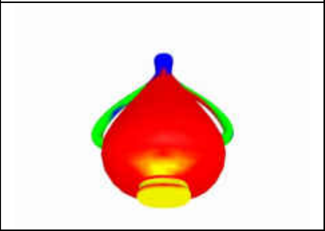	83.95%
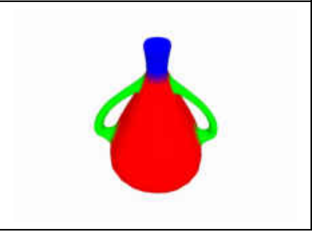	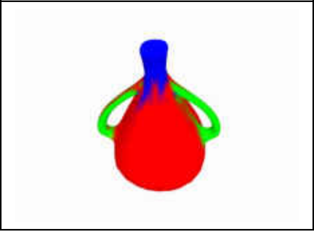		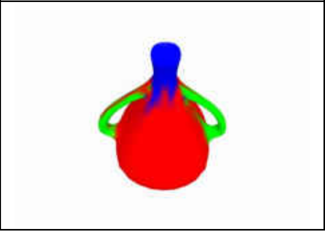	

Table 3 Visualization of Three samples from the Vases test set

6.5. Limitations

Although the Shape Fully Convolutional Network can complete the segmentation task effectively, it still has some limitations. Firstly, the convolution operation has an advantage in extract and highlight the abstract features from the raw data. But because the coordinates and the normal of faces are defined locally for each surface mesh, which can not be used to feed the network. The geometric features used to feed the network must be preprocessed, and most of them are computational heavy. Secondly, the generating layer uses the breadth-first graph search algorithm to find neighbors, and then all the neighbors are sorted by the L2 similarity in the feature dimension. When using a larger neighborhood window, which neighbor is chosen may not consistent across all samples, and the sorting for coarsened graph after each pooling stage makes this even more unstable. In other words, adding more convolution operation at each stage like the U-net [13] is not practical. Finally, to obtain better parameter sharing, the Shape Fully Convolutional Network may need all meshes to be the same triangulation granularity. In other words, the model will work better if triangles across all meshes have similar size, and the number of triangles for each mesh is close to each other.

7. Conclusion

This thesis introduces an implementation of the Shape Fully Convolution Network architecture, which can automatically carry out triangles-to triangles learning and prediction on 3D surface meshes, and complete the segmentation task in a reasonable quality. The Shape Fully Convolution Network is a modification of the Fully Convolutional Network, which shows a good result in image segmentation. It applies the graph convolution and pooling operation [17] for the down-sampling path on the surface mesh by converting the mesh into a general graph structure with each triangle as a node and neighborhood relationships as edges. Then all the nodes are re-ordered based on the multi-layer graph coarsening algorithm [17], which allows the pooling operation to be applied as easily as a 1D pooling. Then a novel generating operation is proposed before each convolution layer. It will generation neighbors for each node, and sort them based on the L2 similarity, which makes the convolution operation more stable. Moreover, the skip architecture similar to the Fully Convolution Network is applied to pass the features from the down-sampling path to the up-sampling path so that more accurate segmentation results can be produced. The experiment shows that the Shape Fully Convolutional Network can predict the edge between two labels quite well. Finally, the multi-label graph cut algorithm [32] is applied to optimize the segmentation results obtained by the network prediction. However, the experiment result shows that the improvement is not significant.

References

[1] Yu, Yizhou; Zhou, Kun; Xu, Dong; Shi, Xiaohan; Bao, Hujun; Guo, Baining; Shum, Heung-Yeung;, "Mesh editing with poisson-based gradient field manipulation," *ACM Transactions on Graphics,* vol. 23, no. 3, pp. 644-651, 2004.

[2] Yang, Yin; Xu, Weiwei; Guo, Xiaohu; Zhou, Kun; Guo, Baining;, "Boundary-Aware Multidomain Subspace Deformation," *IEEE TRANSACTIONS ON VISUALIZATION AND COMPUTER GRAPHICS,* vol. 19, no. 10, pp. 1633-45, 2013.

[3] Chen, Xiaowu; Zhou, Bin; Lu, Feixiang; Wang, Lin; Bi, Lang; Tan, Ping;, "Garment Modeling with a Depth Camera," *ACM Transactions on Graphics,* vol. 34, no. 6, 2015.

[4] Goodfellow, Ian; Bengio, Yoshua; Courville, Aaron;, Deep Learning, MIT Press, 2016.

[5] Krizhevsky, Alex; Sutskever, Ilya; Hinton, Geoffrey E.;, "ImageNet Classification with Deep Convolutional Neural Networks," in *Neural Information Processing Systems (NIPS)*, 2012.

[6] Szegedy, Christian; Liu, Wei; Jia, Yangqing; Sermanet, Pierre; Reed, Scott; Anguelov, Dragomir;, "Going deeper with convolutions," in *2015 IEEE Conference on Computer Vision and Pattern Recognition (CVPR)*, Boston, MA, USA, 2015.

[7] Simonyan, Karen; Zisserman, Andrew;, "Very Deep Convolutional Networks for Large-Scale Image Recognition," *CoRR,* vol. abs/1409.1556, 2014.

[8] Ciresan, Dan; Giusti, Alessandro; Gambardella, Luca M.; Schmidhuber, Jürgen;, "Deep Neural Networks Segment Neuronal Membranes in Electron Microscopy Images," in *Neural Information Processing Systems (NIPS*, 2012.

[9] Farabet, Clement; Couprie, Camille; Najman, Laurent; LeCun, Yann;, "Learning Hierarchical Features for Scene Labeling," *IEEE Transactions on Pattern Analysis and Machine Intelligence,* vol. 35, no. 8, pp. 1915 - 1929, 2013.

[10] Pinheiro, Pedro; Collobert, Ronan;, "Recurrent Convolutional Neural Networks for Scene Parsing," *31st International Conference on Machine Learning,* vol. 1, 2014.

[11] Long, Jonathan; Shelhamer, Evan; Darrel, Trevor;, "Fully Convolutional Networks for Sementic Segmentation," 2015.

[12] Hyeonwoo Noh; Seunghoon Hong; Bohyung Han, "Learning Deconvolution Network for Semantic Segmentation," *CoRR,* vol. abs/1505.04366, 2015.

[13] Olaf Ronneberger; Philipp Fischer; Thomas Brox, "U-Net: Convolutional Networks for Biomedical Image Segmentation," *CoRR,* vol. abs/1505.04597, 2015.

[14] Wang, Pengyu; Gan, Yuan; Shui, Panpan; Yu, Fenggen; Zhang, Yan; Chen, Songle; Sun, Zhengxing, "3D Shape Segmentation via Shape Fully Convolutional Networks," *Computers & Graphics,* vol. 70, no. 2, pp. 128-139, 2018.

[15] Edwards, Michael; Xie, Xianghua;, "Graph Based Convolutional Neural Network," in *BMVC*, 2016.

[16] M. Niepert, M. Ahmed and K. Kutzkov, "Learning Convolutional Neural Networks for Graphs," in *ICML*, 2016.

[17] Deferrard, Michael; Bresson, Xavier; Vandergheynst, Pierre;, "Convolutional Neural Networks on Graphs with Fast Localized Spectral Filtering," 2016.

[18] Xie, Saining; Tu, Zhuowen;, "Holistically-Nested Edge Detection," in *2015 IEEE International Conference on Computer Vision (ICCV)*, 2015.

[19] Liu, Fayao; Shen, Chunhua; Lin, Guosheng; Reid, Ian;, "Learning Depth from Single Monocular Images Using Deep Convolutional Neural Fields," *IEEE Transactions on Pattern Analysis and Machine Intelligence,* vol. 38, pp. 2024-2039, 2016.

[20] Fischer, Philipp; Dosovitskiy, Alexey; Ilg, Eddy; Hausser, Philip; Hazirbacs, Caner; Golkov, Vladimir; Smagt, Patrick van der; Cremers, Daniel; Brox, Thomas;, "FlowNet: Learning Optical Flow with Convolutional Networks," *IEEE International Conference on Computer Vision (ICCV),* pp. 2758-2766, 2015.

[21] Simo-Serra, Edgar; Iizuka, Satoshi; Sasaki, Kazuma; Ishikawa, Hiroshi;, "Learning to Simplify: Fully Convolutional Networks for Rough Sketch Cleanup," *ACM Transactions on Graphics (SIGGRAPH),* vol. 35, no. 4, 2016.

[22] Bruna, Joan; Zaremba, Wojciech; Szlam, Arthur; LeCun, Yann;, "Spectral Networks and Locally Connected Networks on Graphs," *CoRR,* vol. abs/1312.6203, 2013.

[23] Duvenaud, David; Maclaurin, Dougal; Aguilera-Iparraguirre, Jorge; Gómez-Bombarelli, Rafael; Hirzel, Timothy; Aspuru-Guzik, Alán; Adams, Ryan P.;, "Convolutional networks on graphs for learning molecular fingerprints," *Proceeding,* vol. 2, pp. 2224-2232 , 2015.

[24] Wu, Zhirong; Song, Shuran; Khosla, Aditya; Yu, Fisher; Zhang, Linguang; Tang, Xiaoou; Xiao, Jianxiong;, "3D ShapeNets: A deep representation for volumetric

shapes," in *IEEE Conference on Computer Vision and Pattern Recognition (CVPR)*, Boston, MA, USA, 2015.

[25] Qi, Charles Ruizhongtai; Su, Hao; Nießner, Matthias; Dai, Angela; Yan, Mengyuan; Guibas, Leonidas J.;, "Volumetric and Multi-view CNNs for Object Classification on 3D Data," *IEEE Conference on Computer Vision and Pattern Recognition (CVPR),* pp. 5648-5656, 2016.

[26] Kalogerakis, Evangelos; Averkiou, Melinos; Maji, Subhransu; Chaudhuri, Siddhartha;, "3D Shape Segmentation with Projective Convolutional Networks," in *IEEE Computer Vision and Pattern Recognition (CVPR)*, 2017.

[27] Yi, Li; Su, Hao; Guo, Xingwen; Guibas, Leonidas;, "Synchronized Spectral CNN for 3D Shape Segmentation," *10.1109/CVPR.2017.697,* pp. 6584-6592, 2017.

[28] Charles, R. Qi; Su, Hao; Kaichun, Mo; Guibas, Leonidas J.;, "PointNet: Deep Learning on Point Sets for 3D Classification and Segmentation," in *IEEE Conference on Computer Vision and Pattern Recognition*, Honolulu, HI, USA, 2017.

[29] Masci, Jonathan; Boscaini, Davide; Bronstein, Michael M.; Vandergheynst, Pierre;, "Geodesic Convolutional Neural Networks on Riemannian Manifolds," in *IEEE International Conference on Computer Vision Workshop (ICCVW)*, Santiago, Chile , 2015.

[30] Boscaini, Davide; Masci, Jonathan; Rodolà, Emanuele; Bronstein, Michael M.;, "Learning shape correspondence with anisotropic convolutional neural networks," in *Computer Vision and Pattern Recognition*, 2016.

[31] Monti, Federico; Boscaini, Davide; Masci, Jonathan; Rodolà, Emanuele; Svoboda, Jan; Bronstein, Michael M.;, "Geometric Deep Learning on Graphs and Manifolds Using Mixture Model CNNs," in *IEEE Conference on Computer Vision and Pattern Recognition (CVPR)*, Honolulu, HI, USA, 2017.

[32] Boykov, Yuri; Veksler, Olga; Zabih, Ramin;, "Fast approximate energy minimization via graph cuts," *IEEE Transactions on Pattern Analysis and Machine Intelligence ,* vol. 23, no. 11, pp. 1222 - 1239, 2001.

[33] Bui, Thang Nguyen; Jones, Curt;, "Finding good approximate vertex and edge partitions is NP-hard," *Information Processing Letters,* vol. 42, no. 3, pp. 153-159, 1992.

[34] Dhillon, Inderjit S.; Guan, Yuqiang; Kulis, Brian;, "Weighted Graph Cuts without Eigenvectors A Multilevel Approach," *IEEE Transactions on Pattern Analysis and Machine Intelligence,* vol. 29, no. 11, pp. 1944 - 1957, 2007.

[35] C. M. Bishop, Pattern Recognition and Machine Learning, New York: Springer-Verlag, 2006, p. 229.

[36] Gal, Ran; Cohen-Or, Daniel;, "Salient geometric features for partial shape matching and similarity," *ACM Transactions on Graphics (TOG),* vol. 25, no. 1, pp. 130-150, 2006.

[37] L. Shapira; S. Shalom; A. Shamir; D. Cohen-Or; H. Zhang, "Contextual Part Analogies in 3D Objects," *International Journal of Computer Vision,* vol. 89, no. 2-3, p. 309–326, 2010.

[38] Liu, Rong; Zhang, Hao; Shamir, Ariel; Cohen-Or, and Daniel;, "A Part-aware Surface Metric for Shape Analysis," *Computer Graphics Forum,* vol. 28, no. 2, pp. 397-406, 2009.

[39] Hilaga, Masaki; Shinagawa, Yoshihisa; Kohmura, Taku; Kunii, Tosiyasu L.;, "Topology matching for fully automatic similarity estimation of 3D shapes," *Proceeding,* pp. 203-212 , 2001.

[40] Belongie, Serge; Malik, Jitendra; Puzicha, Jan;, "Shape matching and object recognition using shape contexts," *IEEE Transactions on Pattern Analysis and Machine Intelligence,* vol. 24, no. 4, pp. 509 - 522, 2002.

[41] Johnson, Andrew E.; Hebert, Martial;, "Using spin images for efficient object recognition in cluttered 3D scenes," *IEEE Transactions on Pattern Analysis and Machine Intelligence,* vol. 21, no. 5, pp. 433 - 449, 1999.

[42] Guo, Kan; Zou, Dongqing; Chen, Xiaowu;, "3D Mesh Labeling via Deep Convolutional Neural Networks," *ACM Transactions on Graphics,* vol. 35, no. 3, 2015.

[43] Wang, Yunhai; Asafi, Shmulik; van Kaick, Oliver; Zhang, Hao; Cohen-Or, Daniel; Chen, Baoquan;, "Active Co-analysis of a Set of Shapes," *ACM Transactions on Graphics (TOG),* vol. 31, no. 6, pp. 165:1--165:10, 2012.